Electronic Supplementary Material (ESI) for Journal of Materials Chemistry C.

Supplementary Information for:

Homoleptic Zirconium Amidates: Single Source Precursors for the Aerosol-assisted Chemical Vapour Deposition of ZrO_2

Amanda L. Catherall, Michael S. Hill, Andrew L. Johnson, Gabriele Kociok-Köhn and Mary F. Mahon

General Techniques. All reactions were carried out using standard Schlenk line and glovebox techniques under an inert atmosphere of argon and nitrogen, respectively. Tetrahydrofuran (THF) was dried over potassium before isolating via distillation. Hexanes and toluene solvents were dried using a commercially available solvent purification system (Innovative Technology Inc., Amesbury, MA, USA) and all solvents were degassed under argon prior to use. Deuterated toluene NMR solvent was purchased from Fluorochem, Hadfield, U.K., and dried over potassium before isolating via vacuum distillation. All dry solvents were stored under argon in Young's ampules over 4 Å molecular sieves. All reagents were purchased from Sigma-Aldrich and used as supplied. The starting material tetrakis(dimethylamido)zirconium was synthesised according to literature procedure.[1]

General procedure for preparation of amide pro-ligands

Amine and triethylamine were solubilised in diethylether and stirred at room temperature for 30 minutes. The appropriate acyl chloride was then added dropwise to the amine solution and the colourless precipitate was removed by filtration. The solvent was removed in vacuo to provide the amide product.

***N-tert*-butylpivalamide:** *t*-butylamine (4.65 ml, 44.40 mmol), triethylamine (6.17 ml, 44.40 mmol) and pivaloyl chloride (5.21 ml, 42.30 mmol) Yield: White solid, no further purification needed (6.64 g, 76%) ^{1}H NMR ($CDCl_3$, 300MHz, 294.4K) δ (ppm): 5.41 (bs, NH, 1H) 1.33 (s, CH_3, 9H) 1.16 (s, CH_3, 9H) ^{13}C{^{1}H} NMR ($CDCl_3$, 75MHz, 294.5K) δ (ppm): 177.78 (*C*O) 50.63 ($\mathit{C}(CH_3)_3$) 38.62 ($NH\mathit{C}(CH_3)_3$) 28.69 ($\mathit{C}H_3$) 27.63 ($\mathit{C}H_3$) HRMS (ESI) Calculated for $C_9H_{19}NO$ expected m/z 157.15 found [M+H] 158.1544 [M+Na] 180.1368.

***N-tert*-butyl-2-methylpropanamide:** *tert*-butylamine (5.22 ml, 49.35 mmol), triethylamine (6.87 ml, 49.35 mmol) and *iso*-butyl chloride (4.91 ml, 47.00 mmol) Yield: White solid, no further purification needed (5.37 g, 80 %) ^{1}H NMR (C_6D_6, 300MHz, 294.4K) δ (ppm): 5.02 (bs, NH, 1H) 1.90 (m, CH, 1H) 1.56 (s, CH_3, 1H) 1.06 (d, J_{HH} = 6.8 Hz, CH_3, 6H) ^{13}C{^{1}H} NMR (C_6D_6, 75MHz, 294.5K) δ (ppm): 176.1 (*C*O) 50.8 (C(*C*H$_3$)$_3$) 36.6 (*C*H(CH$_3$)$_2$) 29.2 (C(*C*H$_3$)$_3$) 20.3 (CH(*C*H$_3$)$_2$) HRMS (ESI) Calculated for $C_8H_{17}NO$ expected m/z 143.13 found [M+Na] 166.1202.

***N*-*iso*propylpivalamide:** *Iso*-propylamine (3.76 ml, 43.90 mmol), triethylamine (6.12 ml, 43.90 mmol) and pivaloyl chloride (5.15 ml, 41.90 mol) Yield: White solid, no further purification needed (4.78g, 80%) ^{1}H NMR (CDCl$_3$, 300MHz, 294.4K) δ (ppm): 5.38 (bs, NH, 1H) 4.05 (m, CH, 1H) 1.78 (s, CH$_3$, 1H) 1.18 (s, CH$_3$, 9H) 1.14 (d, J_{HH} = 6.6 Hz, CH$_3$, 6H) ^{13}C{^{1}H} NMR (CDCl$_3$, 75MHz, 294.5K) δ (ppm): 177.51 (*C*O) 41.08 (*C*H) 38.43 (*C*H) 27.54 (*C*(CH$_3$)$_3$) 22.73 (*C*H$_3$) HRMS (ESI) Calculated for $C_8H_{17}NO$ expected m/z 143.13 found [M+H] 144.1401 [M+Na] 166.1219.

2-methyl-*N*-(propan-2-yl)propanamide: *iso*-propylamine (4.00 ml, 47.00 mmol), triethylamine (6.54 ml, 47.00 mmol) and *iso*-butyl chloride (4.92 ml, 47.00 mmol) Yield: White solid, no further purification needed (4.94 g, 82 %) ^{1}H NMR (C$_6$D$_6$, 300MHz, 294.4K) δ (ppm): 5.21 (bs, NH, 1H) 4.15 (m, CH, 1H) 1.99 (m, CH, 1H) 1.09 (d, J_{HH} = 6.8 Hz, CH$_3$, 6H) 0.92 (d, J_{HH} = 6.6 Hz, CH$_3$, 6H) ^{13}C{^{1}H} NMR (C$_6$D$_6$, 75MHz, 294.5K) δ (ppm): 175.73 (*C*O) 41.29 (N*C*(CH$_3$)$_3$) 35.94 (*C*(CH$_3$)$_3$) 23.02 (NC(*C*H$_3$)$_3$) 20.27 (C(*C*H$_3$)$_3$) HRMS (ESI) Calculated for $C_7H_{15}NO$ expected m/z 129 found [M+Na] 152.1010.

***N*-*tert*-butylpropanamide:** *tert*-butylamine (5.67 ml, 54.00 mmol), triethylamine (7.51 ml, 54.00 mmol) and propionyl chloride (4.72 ml, 54.00 mmol) Yield: White solid, no further purification needed (5.41 g, 78 %) ^{1}H NMR (C$_6$D$_6$, 300MHz, 294.4K) δ (ppm): 4.95 (bs, NH, 1H) 1.78 (q, CH$_2$, J = 7.6 Hz, 2H) 1.25 (s, CH$_3$, 9H) 1.05 (t, CH$_3$, J=7.5 Hz, 3H) ^{13}C{^{1}H} NMR (C$_6$D$_6$, 75MHz, 294.5K) δ (ppm): 172.7 (*C*O) 50.9 (*C*(CH$_3$)) 30.7 (*C*H$_2$) 29.1 (C(*C*H$_3$)) 10.5 (*C*H$_3$). HRMS (ESI) Calculated for $C_7H_{15}NO$ expected m/z 129 found [M+Na].

***N*-(propan-2-yl)propanamide:** *iso*-propylamine (4.59 ml, 54.00 mmol), triethylamine (7.51 ml, 54.00 mmol) and propionyl chloride (4.72 ml, 54.00 mmol) Yield: White solid, no further purification needed (4.99 g, 80 %) ^{1}H NMR (C$_6$D$_6$, 300MHz, 294.4K) δ (ppm): 6.34 (bs, NH, 1H) 4.18 (sept, J_{HH} = 7.76 Hz, CH, 1H) 2.04 (q, CH$_2$, J = 7.41 Hz, 2H) 1.12 (t, J_{HH} =7.76 Hz, CH$_3$, 3H) 1.02 (d, CH$_3$, J = 6.0 Hz, 3H) ^{13}C{^{1}H} NMR (C$_6$D$_6$, 75MHz, 294.5K) δ (ppm): 173.1 (*C*O) 41.5 (*C*H(CH$_3$)$_2$) 30.1 (*C*H$_2$) 23.1 (C(*C*H$_3$)) 10.69 (*C*H$_3$). HRMS (ESI) Calculated for $C_7H_{15}NO$ expected m/z 129 found [M+Na].

***N*-*tert*-butyl-acetamide:** *tert*-butylamine (7.02 ml, 67.20 mmol), triethylamine (9.34 ml, 67.20 mmol) and acetyl chloride (4.56 ml, 64.00 mmol) Yield: White solid, no further purification needed (6.06 g, 82 %) ^{1}H NMR (C$_6$D$_6$, 300MHz, 294.4K) δ (ppm): 5.34 (bs, NH, 1H) 1.61 (s, CH$_3$, 3H) 1.25 (s, CH$_3$, 9H) $^{13}C\{^1H\}$ NMR (C_6D_6, 75MHz, 294.5K) δ (ppm): 169.2 (*C*O) 51.0 (*C*$(CH_3)_3$) 29.12 (C(*C*$H_3)_3$) 24.4 (*C*H_3). HRMS (ESI) Calculated for $C_6H_{13}NO$ expected m/z 115 found [M+Na].

General procedure for preparation of complexes 1 - 6

A solution of tetrakis(dimethylamido)zirconium in toluene was added dropwise to a solution of amide proligand at -78 °C. The reaction mixture was heated at 60 °C for 18 hours. The solvent and volatile by-product were removed *in vacuo* and the product obtained as a solid.

Tris(*N*-*tert*-butyl-2,2-dimethylpropanamidato)dimethylamidozirconium (1)

N-*tert*-butyl-2,2-dimethylpropanamide (1 g, 6.37 mmol) and [Zr($NMe_2)_4$] (0.57 g, 2.12 mmol) in toluene. White solid (0.58 g, 45%). Elemental analysis: calculated for $C_{29}H_{60}N_4O_3Zr$: C, 57.66; H, 10.01; N, 9.28. Found C, 57.50; H, 10.25; N, 9.14. ^1H NMR (C_7D_8, 300 MHz, 294.4 K) δ (ppm): 3.06 (s, 6H, NCH_3), 1.56 (s, 9H, CH_3), 1.45 (s, 9H, CH_3), 1.28 (s, 18H, CH_3), 1.24 (s, 9H, CH_3); $^{13}C\{^1H\}$ NMR (C_7D_8, 75 MHz, 294.5 K) δ (ppm): 165.3 (*C*N), 52.4, 51.7 (N*C*$(CH_3)_3$), 40.9 (N*C*H_3), 40.3, 39.7 (C*C*$(CH_3)_3$), 32.5, 31.0, 29.1 (CH_3). Melting point: 155 – 158 °C.

Tetrakis(*N*-*tert*-butyl-2-methylpropanamidato)zirconium (2)

N-*tert*-butyl-2-methylpropanamide (2.80 g, 10.49 mmol) and [Zr($NMe_2)_4$] (6 g, 41.96 mmol) in toluene. Light yellow/white solid (6.65 g, 96%). Elemental analysis: calculated for $C_{32}H_{64}N_4O_4Zr$: C, 58.23; H, 9.77; N, 8.49. Found C, 57.63; H, 10.39; N, 8.31. ^1H NMR (C_6D_6, 300 MHz, 294.4 K) δ (ppm): 2.78 (sept, $^3J_{HH}$ = 6.6 Hz, 4H, CH), 1.42 (s, 36H, CH_3), 1.23 (d, $^3J_{HH}$ = 6.6 Hz, 24H, CH_3); $^{13}C\{^1H\}$ NMR (C_6D_6, 75 MHz, 294.5 K) δ (ppm): 189.8 (*C*O), 52.6 (*C*CH_3), 33.1 (*C*H), 32.0 (CH_3), 20.3 (CH_3). Melting point: Did not melt up to the decomposition temperature.

Tetrakis(*N*-*tert*-butylpropanamidato)zirconium (3)

N-*tert*-butylpropanamide (0.9678 g, 7.49 mmol) and [Zr($NMe_2)_4$] (0.5 g, 1.87 mmol) in toluene. Light yellow/white solid (1.01 g, 89%). Elemental analysis: calculated for $C_{28}H_{56}N_4O_4Zr$: C, 55.68; H, 9.35; N, 9.28. Found C, 55.29; H, 10.02; N, 9.18. ^1H NMR (C_6D_6, 300 MHz, 294.4 K) δ (ppm): 2.27 (q, $^3J_{HH}$ = 7.5 Hz, 8H, CH_2), 1.38 (s, 36H, CH_3), 1.21 (t, $^3J_{HH}$ = 7.54 Hz, 12H, CH_3); $^{13}C\{^1H\}$ NMR (C_6D_6, 75M Hz, 294.5 K) δ (ppm): 186.0 (*C*O), 52.6 (*C*CH_3), 32.0 (C*C*H_3), 28.6 (CH_2), 10.5 (CH_3). Melting point: Did not melt up to the decomposition temperature.

Tetrakis(*N*-*tert*-butylacetamidato)zirconium (4)

N-*tert*-butylacetamide (0.87 g, 7.52 mmol) and [Zr($NMe_2)_4$] (0.50 g, 1.88 mmol) in toluene. White product (0.78 g, 76%). Elemental analysis: calculated for $C_{24}H_{48}N_4O_4Zr$: C, 52.61; H, 8.83; N, 10.23. Found: C, 52.59; H, 8.96; N, 10.18. ^1H NMR (C_6D_6, 300 MHz, 294.4 K) δ (ppm): 1.90 (s, 12H, CH_3), 1.35 (s, 36H, CH_3); $^{13}C\{^1H\}$ NMR (C_6D_6, 75 MHz, 294.5 K) δ (ppm): 182.5 (*C*O), 52.6 (*C*CH_3), 31.6 (CH_3), 22.7 (CH_3). Melting point: Did not melt up to the decomposition temperature.

Tetrakis(*N*-*iso*propylpivalamidato)zirconium (5)

N-*iso*propylpivalamide (0.20 g, 1.41 mmol) and [Zr(NMe_2)$_4$] (0.09 g, 0.35 mmol) in toluene. White product (0.07 g, 31%). Elemental analysis: calculated for $C_{32}H_{64}N_4O_4Zr$: C, 58.23; H, 9.77; N, 8.49. Found C, 56.10; H, 10.28; N, 8.10. ^1H NMR (C_6D_6, 300 MHz, 294.4 K) δ (ppm): 4.00 (sept, $^3J_{HH}$ = 6.22 Hz, 4H, CH), 1.37 (d, J_{HH} = 6.22 Hz, 24H, CH_3), 1.21 (s, 24H, CH_3). $^{13}C\{^1H\}$ NMR (C_6D_6, 75MHz, 294.5K) δ (ppm): 184.5 (*C*O), 41.4 (*C*CH_3), 37.5 (*C*H), 26.5 (C(*C*H_3)$_3$), 22.6 (CH(*C*H_3)$_2$). Melting point: Did not melt up to the decomposition temperature.

Tetrakis(2-methyl-*N*-(propan-2-yl)propanamide)zirconium (6)

2-methyl-*N*-(propan-2-yl)propanamide (1.92 g, 14.88 mmol) and [Zr(NMe_2)$_4$] (0.98 g, 3.72 mmol) in toluene. Pale yellow solid (2.14 g, 95%). Elemental analysis: calculated for $C_{28}H_{56}N_4O_4Zr$: C, 55.68; H, 9.35; N, 9.28. Found C, 55.60; H, 9.43; N, 9.21. ^1H NMR (C_6D_6, 300 MHz, 294.4 K) δ (ppm): 3.56 (sept, $^3J_{HH}$ = 6.4 Hz, 4H, CH), 2.60 (sept, $^3J_{HH}$ = 6.78 Hz, 4H, CH), 1.33 (d, $^3J_{HH}$ = 6.4 Hz, 24H, CH_3), 1.14 (d, $^3J_{HH}$ = 6.8 Hz, 24H, CH_3); $^{13}C\{^1H\}$ NMR (C_6D_6, 75 MHz, 294.5 K) δ (ppm): 188.7 (*C*O), 48.1 (*C*H), 29.0 (*C*H), 25.0 (CH_3), 19.7 (CH_3). Melting point: Did not melt up to the decomposition temperature.

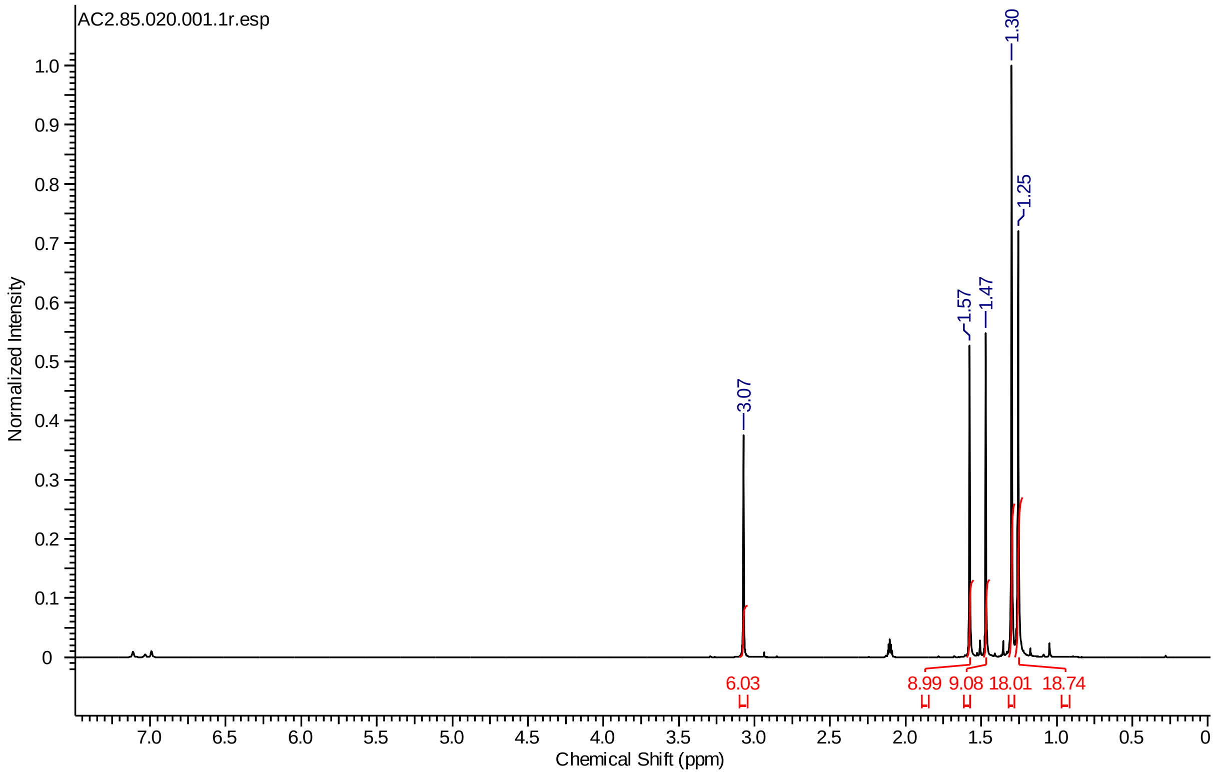

Figure S1: ^{1}H NMR spectrum of compound **1**

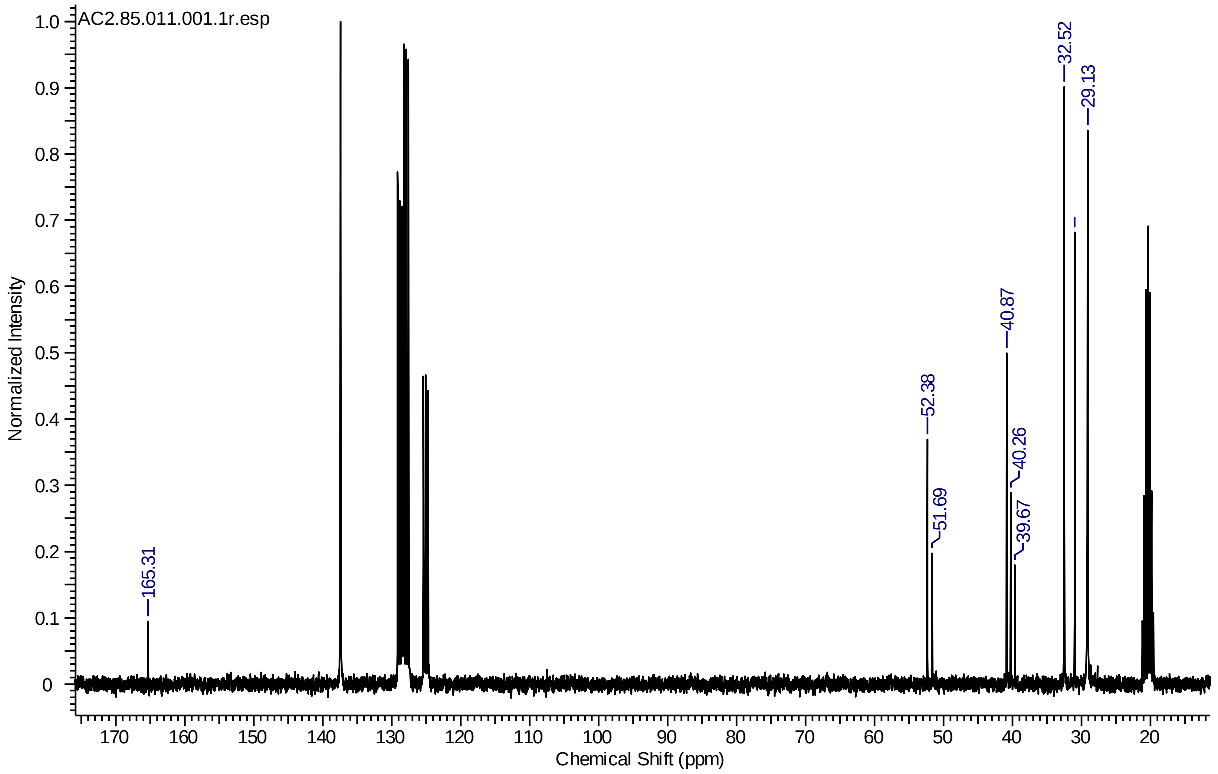

Figure S2: ^{13}C{^{1}H} NMR spectrum of compound **2**

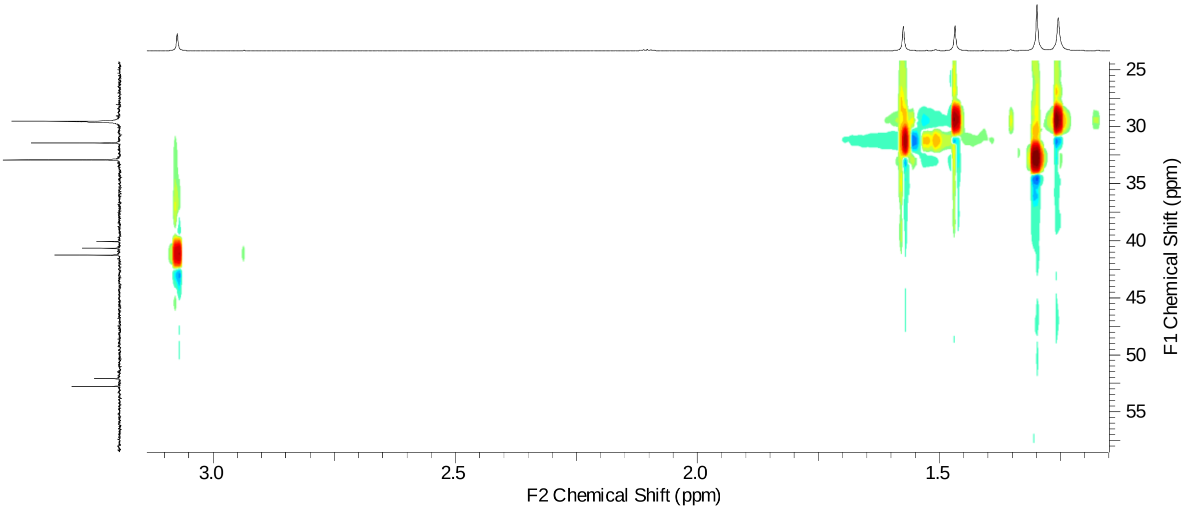

Figure S3: HSQC spectrum of compound **1**

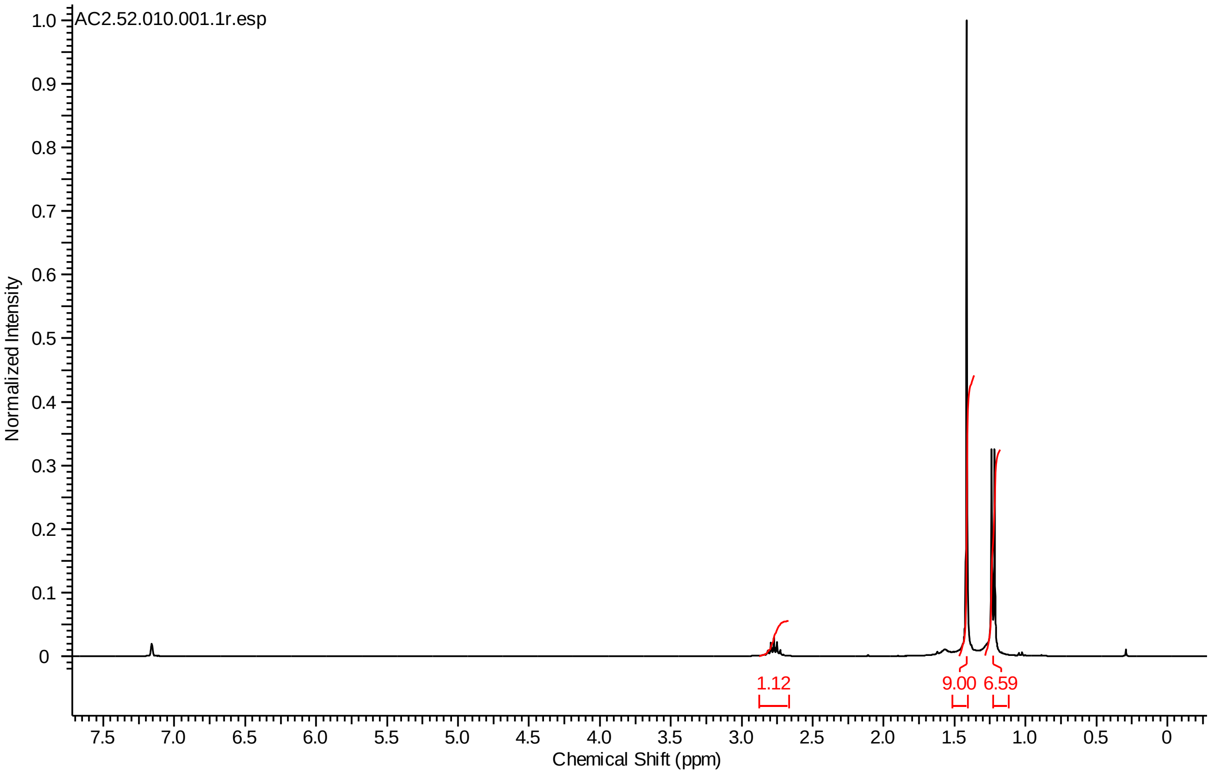

Figure S4: ^{1}H NMR spectrum of compound **2**

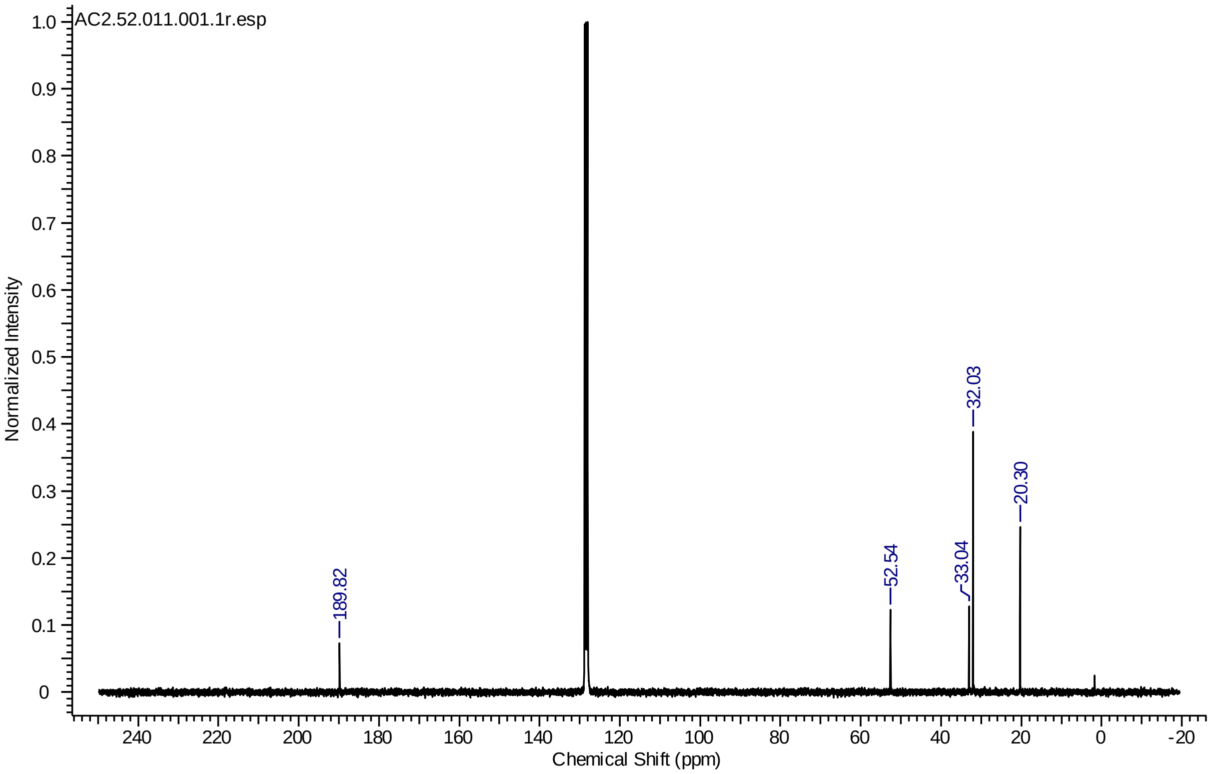

Figure S5: $^{13}C\{^{1}H\}$ NMR spectrum of compound **2**

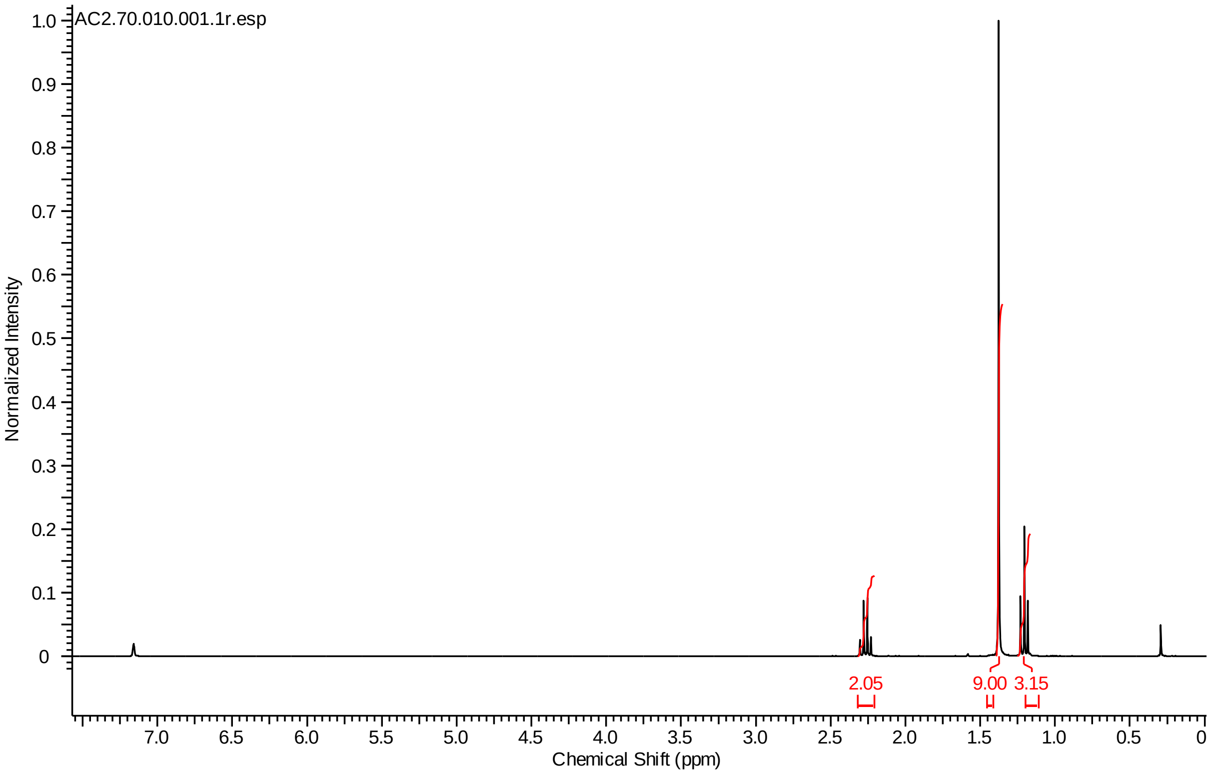

Figure S6: ^{1}H NMR spectrum of compound **3**

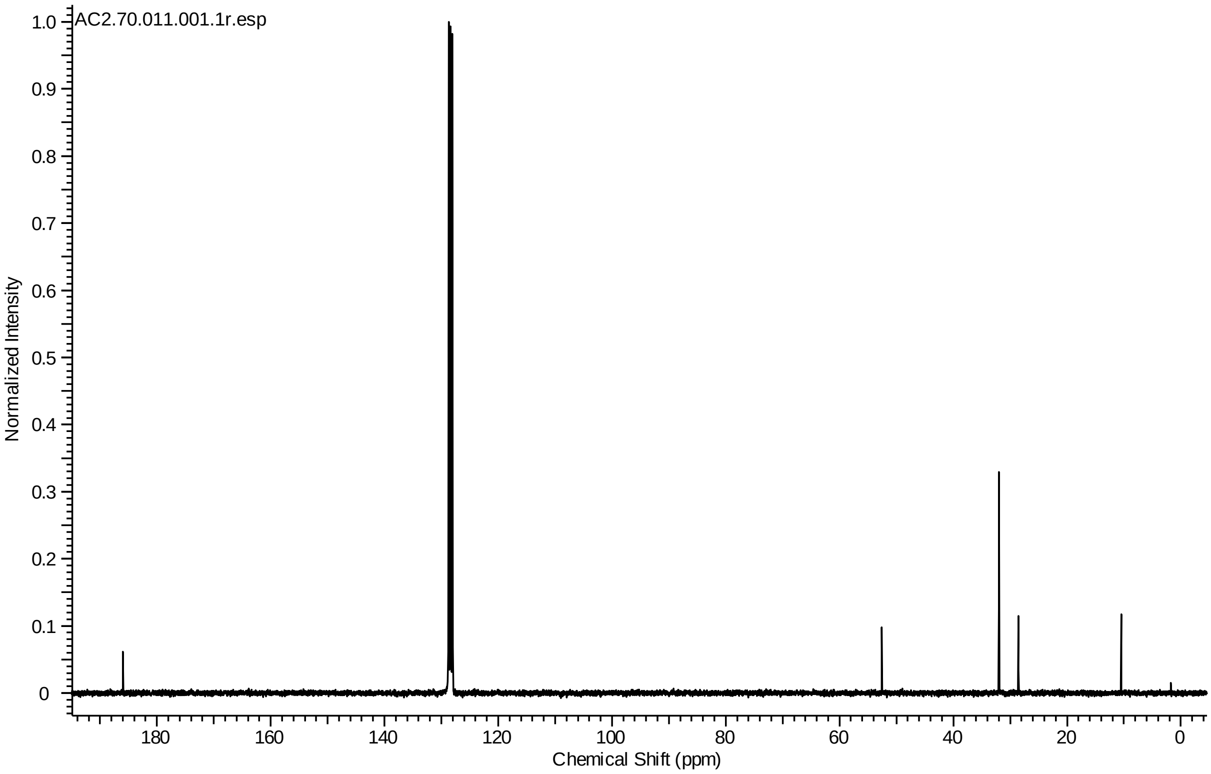

Figure S7: $^{13}C\{^{1}H\}$ NMR spectrum of compound **3**

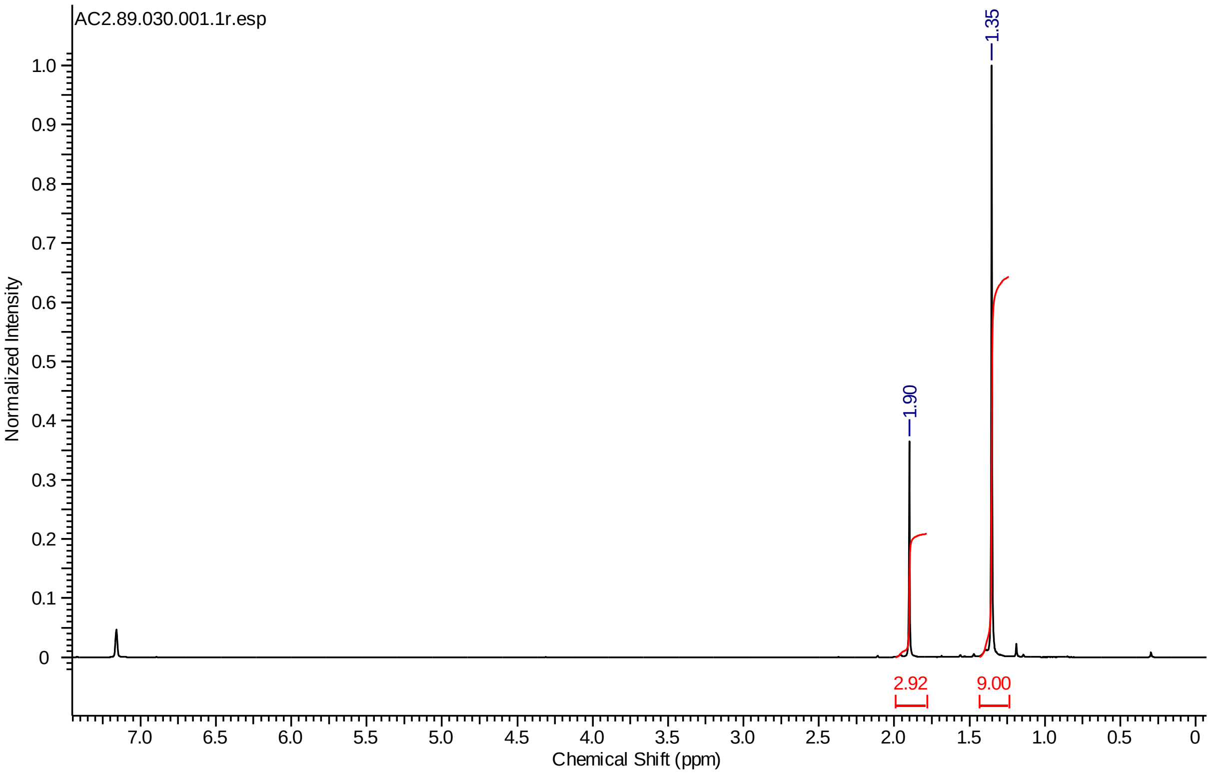

Figure S8: ^{1}H NMR spectrum of compound **4**

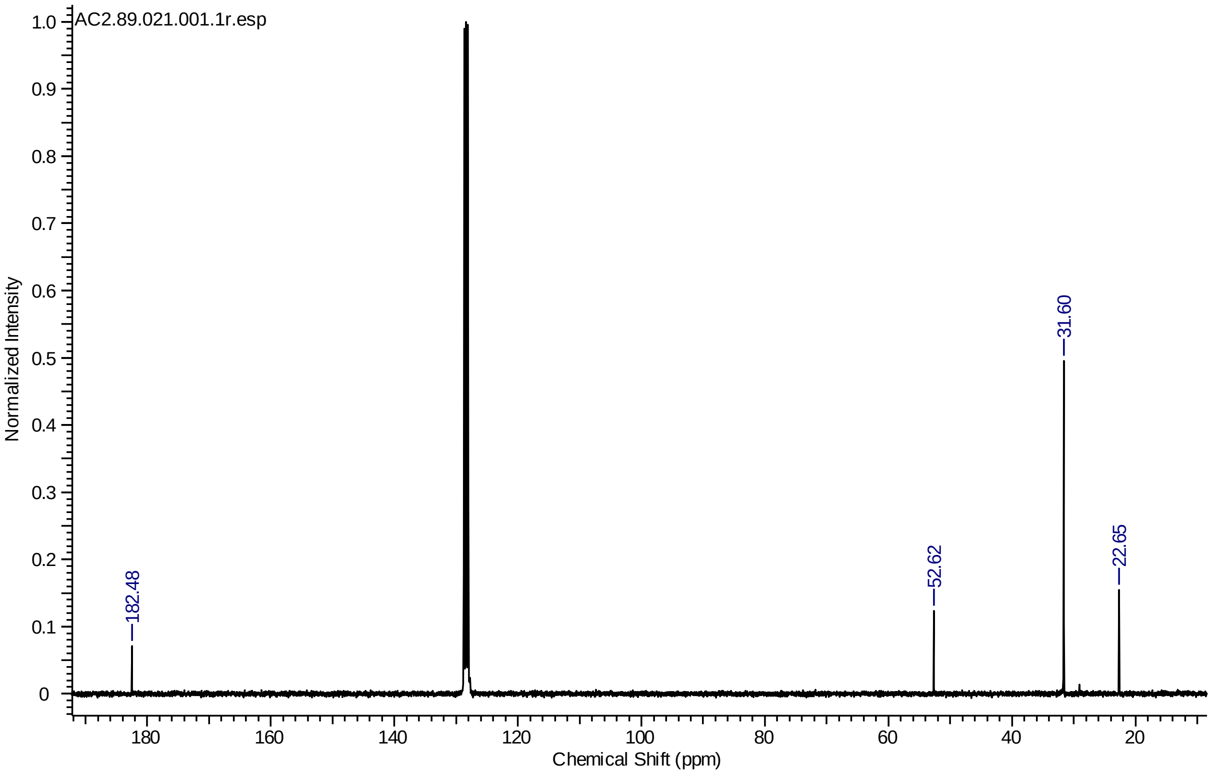

Figure S9: $^{13}C\{^{1}H\}$ NMR spectrum of compound **4**

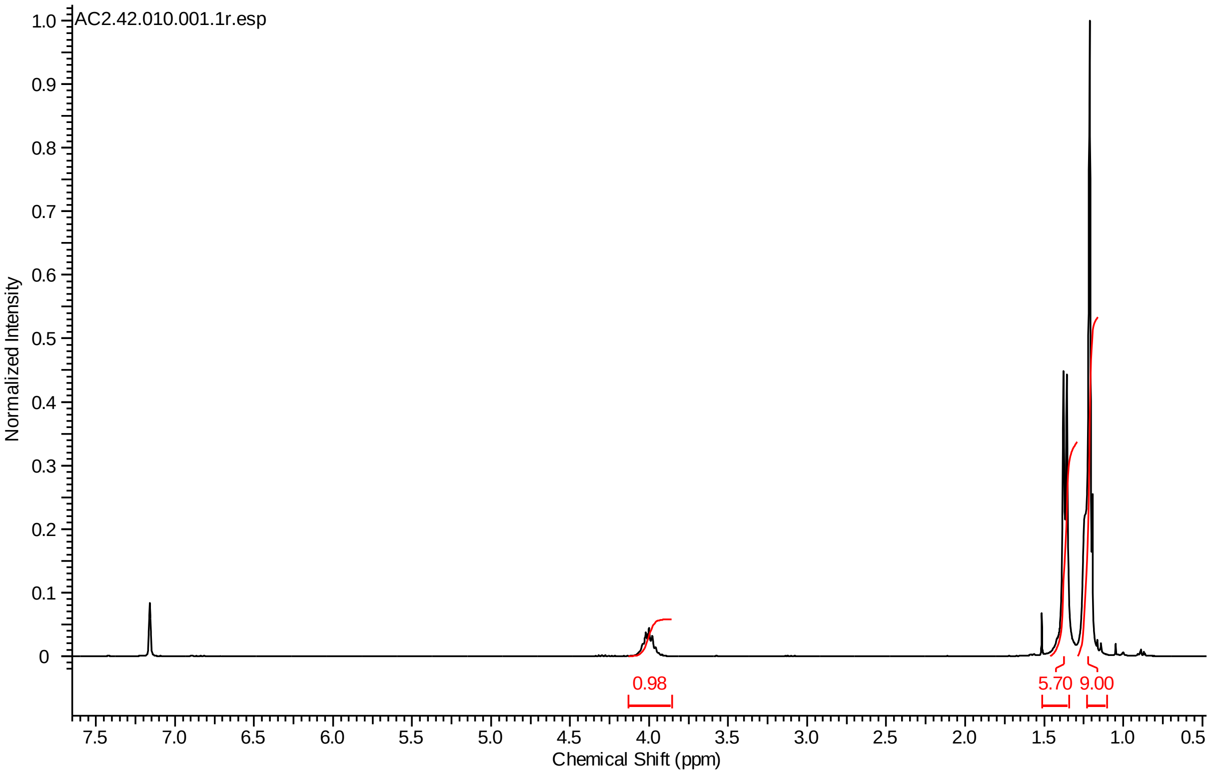

Figure S10: ^{1}H NMR spectrum of compound **5**

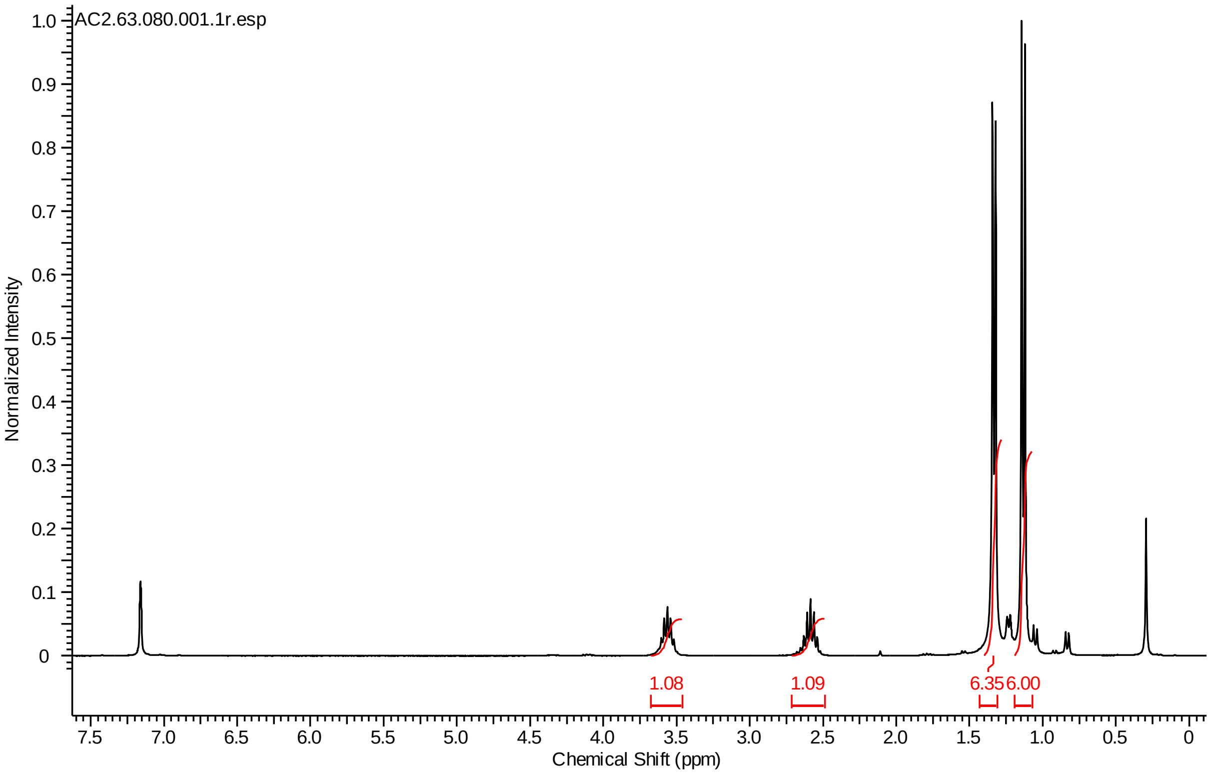

Figure S11: ^{1}H NMR spectrum of compound **6**

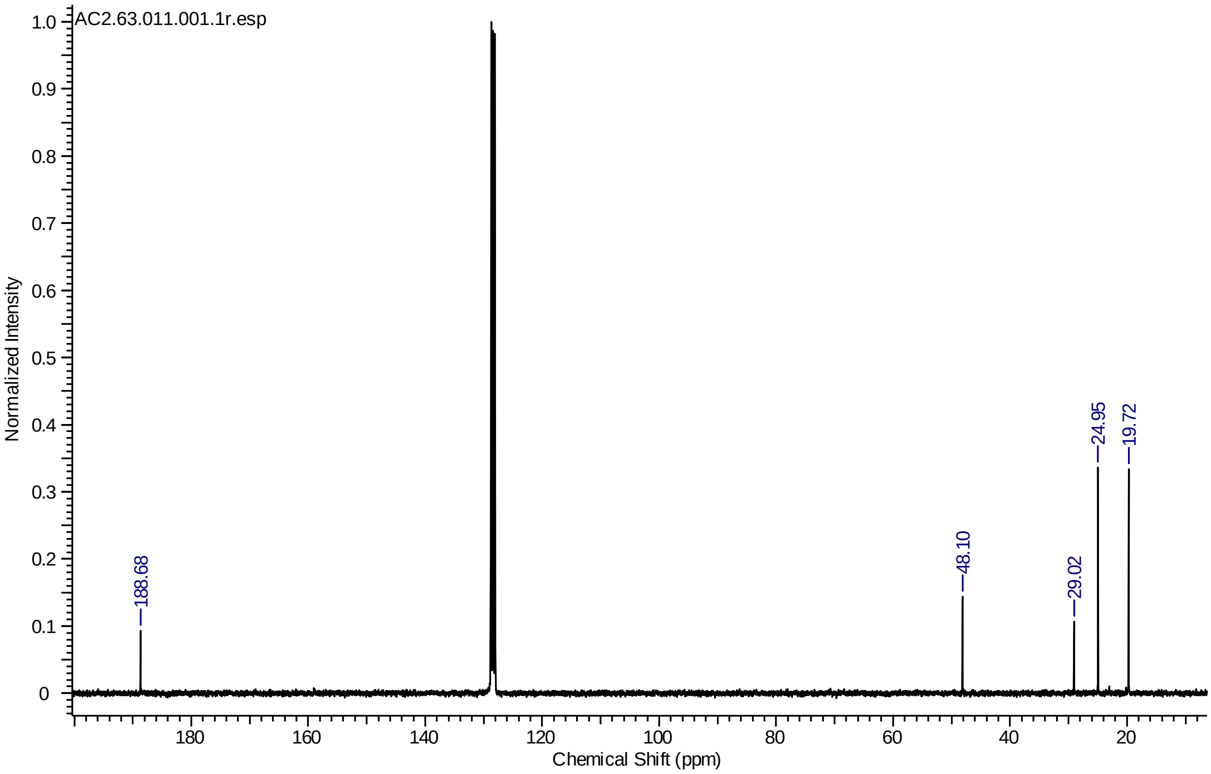

Figure S12: ^{13}C{^{1}H} NMR spectrum of compound **6**

Thermogravimetric Analysis. Thermogravimetric analysis (TGA) was collected using a TGA 4000 PerkinElmer system. Samples were prepared air sensitively using a crimped aluminium sample pan. TGAs were performed under a flow of N_2 at 20 mL min^{-1} and heated from 30 to 600°C at a ramp rate of 5°C min^{-1}.

Thermal Decomposition. In a glovebox a sample of the relevant zirconium amidate (**2**, **5** or **6**, *ca.* 0.1 g) was loaded into a silica tube, which was attached to a three way tap. A J Youngs NMR tap charged with 0.5 mL d_8-toluene was attached to another outlet of the tap and the whole system was sealed and removed for the glove box. The third outlet of the three way tap was attached to a vacuum line, the NMR tube was cooled to –78°C and the entire apparatus was evacuated (ca 10^{-1} mmHg). At this point the silica tube containing the zirconium amidate was placed inside a Carbolite tube furnace and isolated such that the sample and NMR tubes were connected under a static vacuum (Figure S13). Compounds **2** and **5** were heated to 400°C while **6** was heated 350°C for ca. 45 minutes. During this time a colourless solid was observed to form on the exterior cold walls of the silica tube. This was sampled and the NMR tube was sealed for analysis.

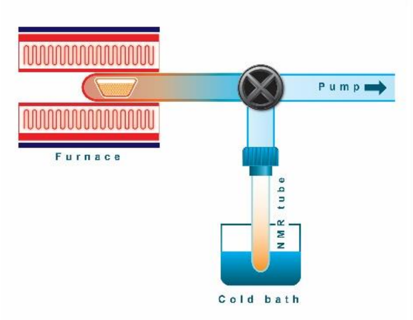

Figure S13: Schematic of the apparatus employed to assess the thermal decomposition of compounds **2**, **5** and **6**.

Figure S14: ^{1}H NMR spectrum (d_8-toluene, 298K) of the volatile products resulting from the thermal decomposition of compound **6**.

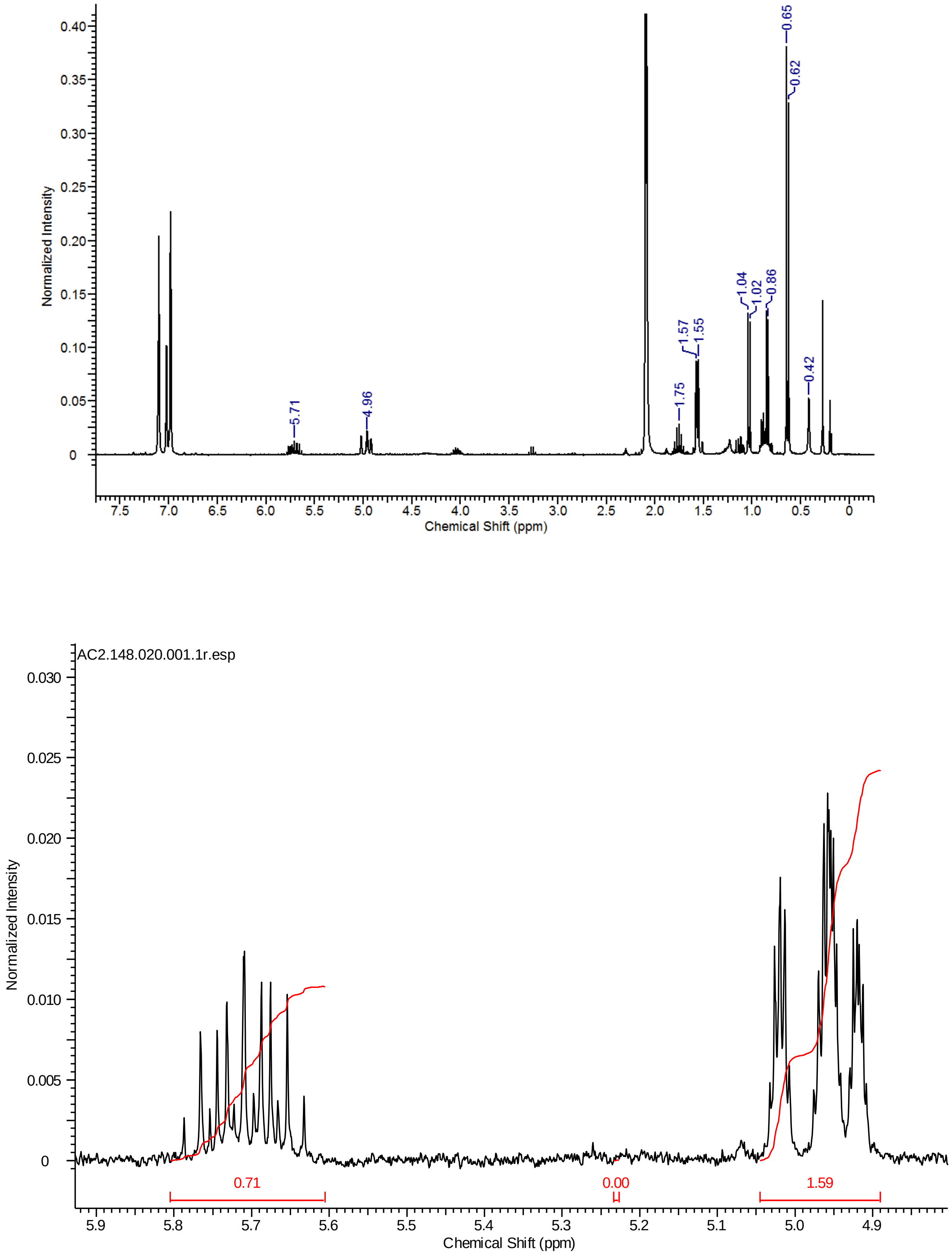

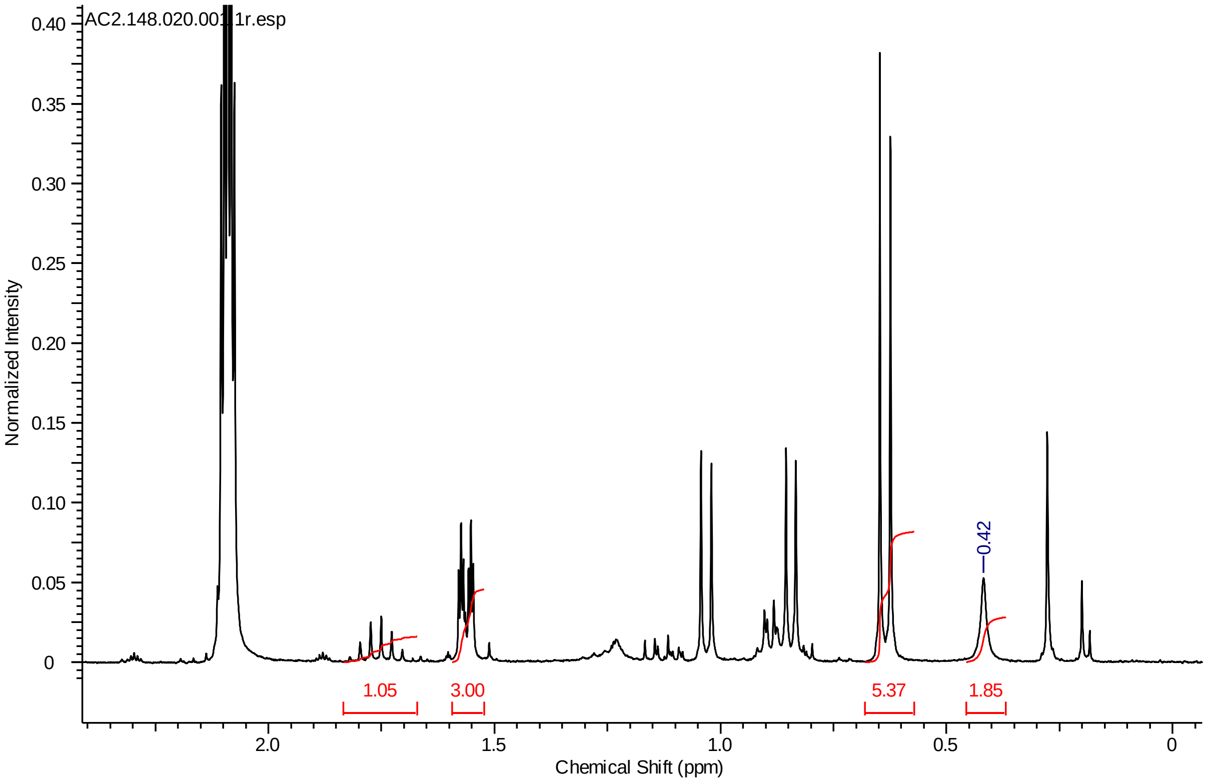

Figure S15: COSY NMR spectrum of the volatile products resulting from the thermal decomposition of compound **6**.

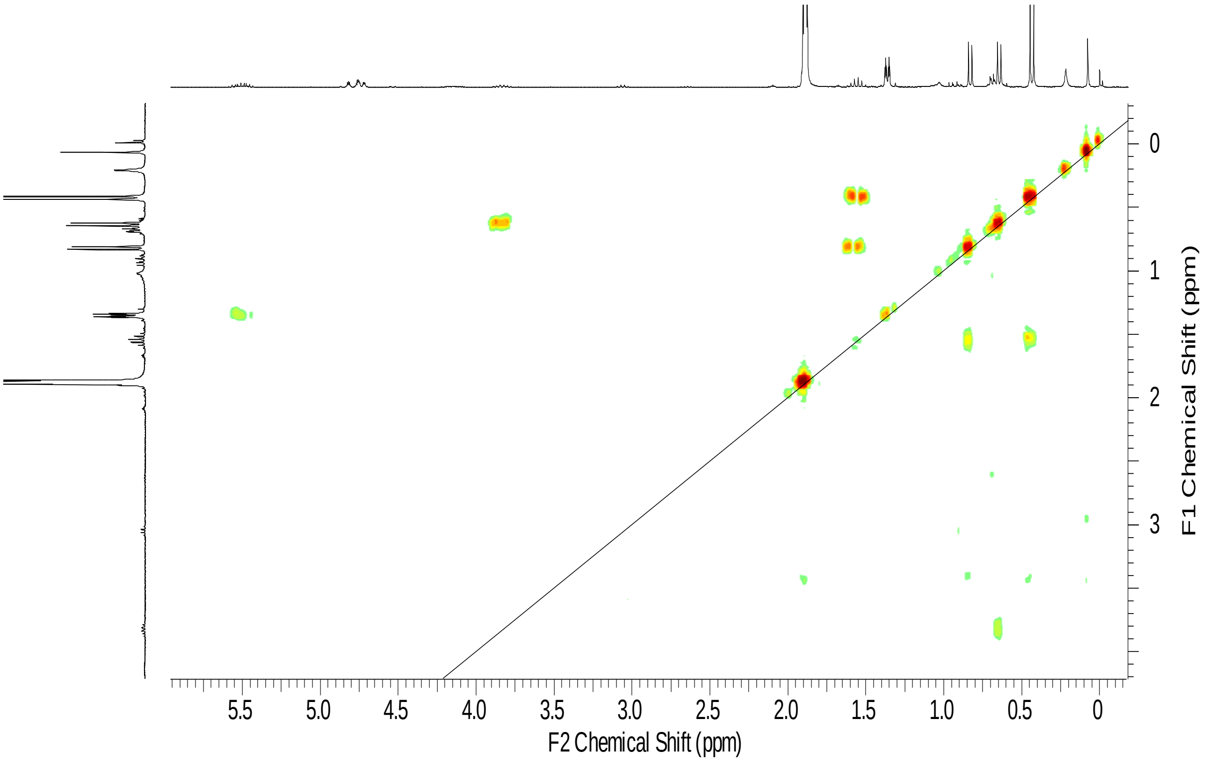

Figure S16: ^{1}H NMR spectrum of the volatile products resulting from the thermal decomposition of compound **2**.

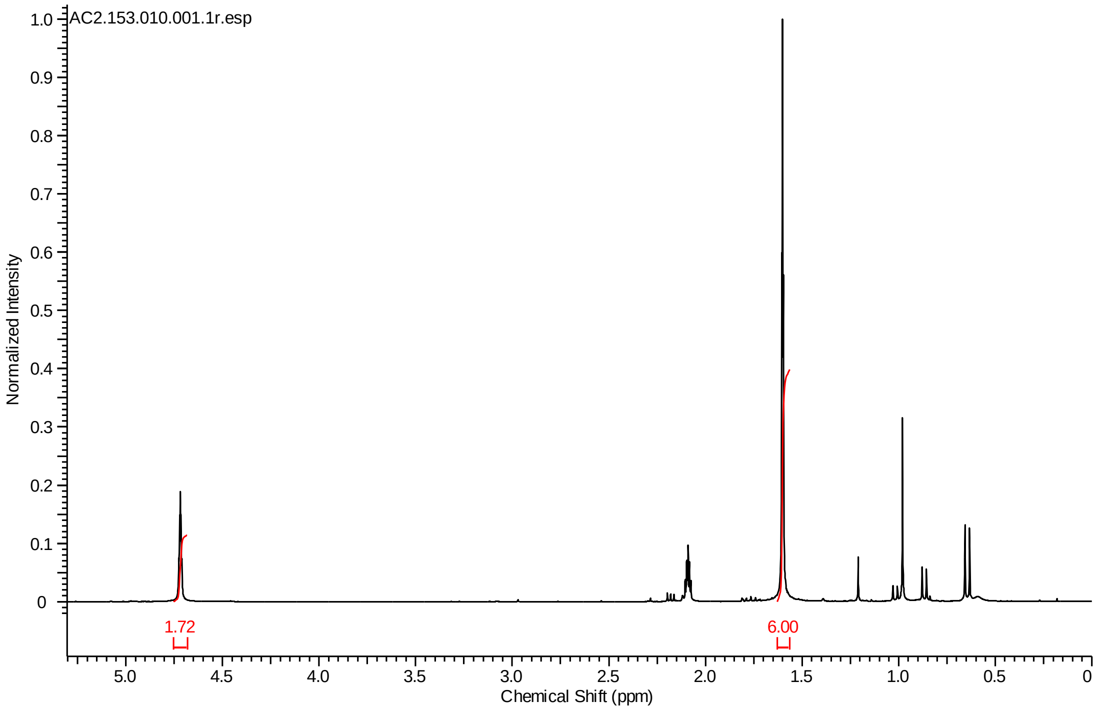

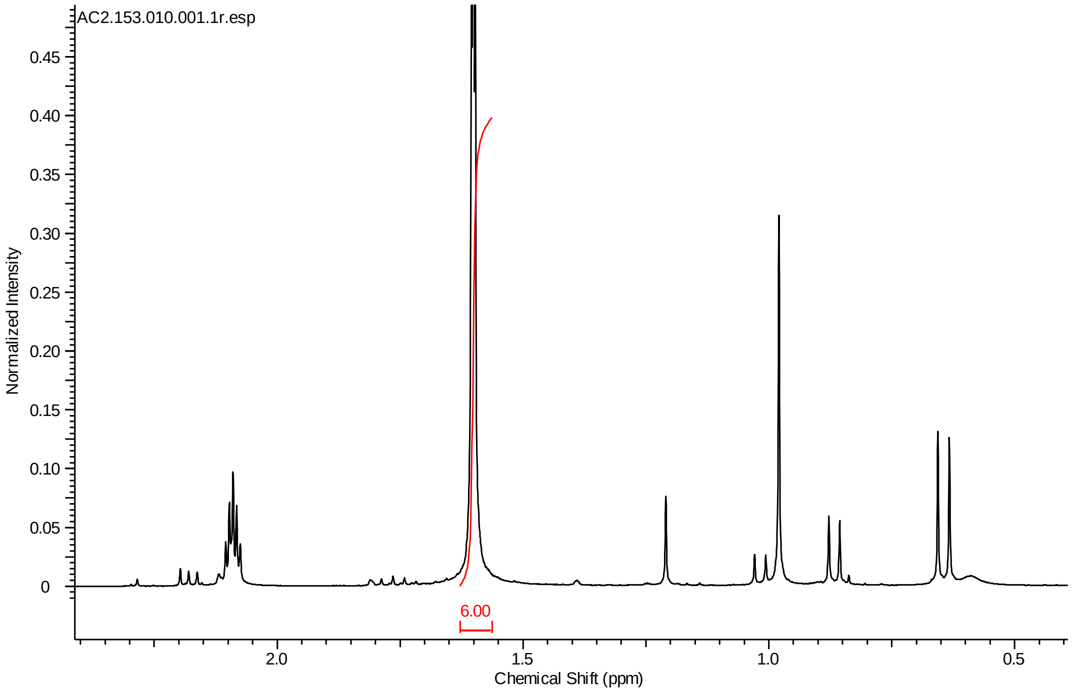

Figure S17: COSY NMR spectrum of the volatile products resulting from the thermal decomposition of compound **2**.

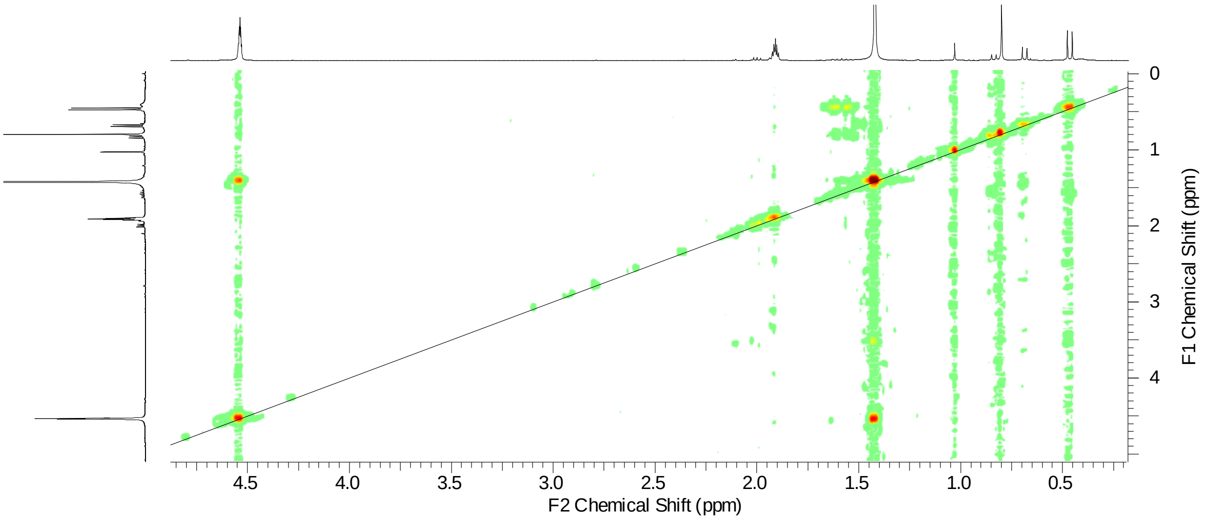

Figure S18: ^{1}H NMR spectrum of the volatile products resulting from the thermal decomposition of compound **5**.

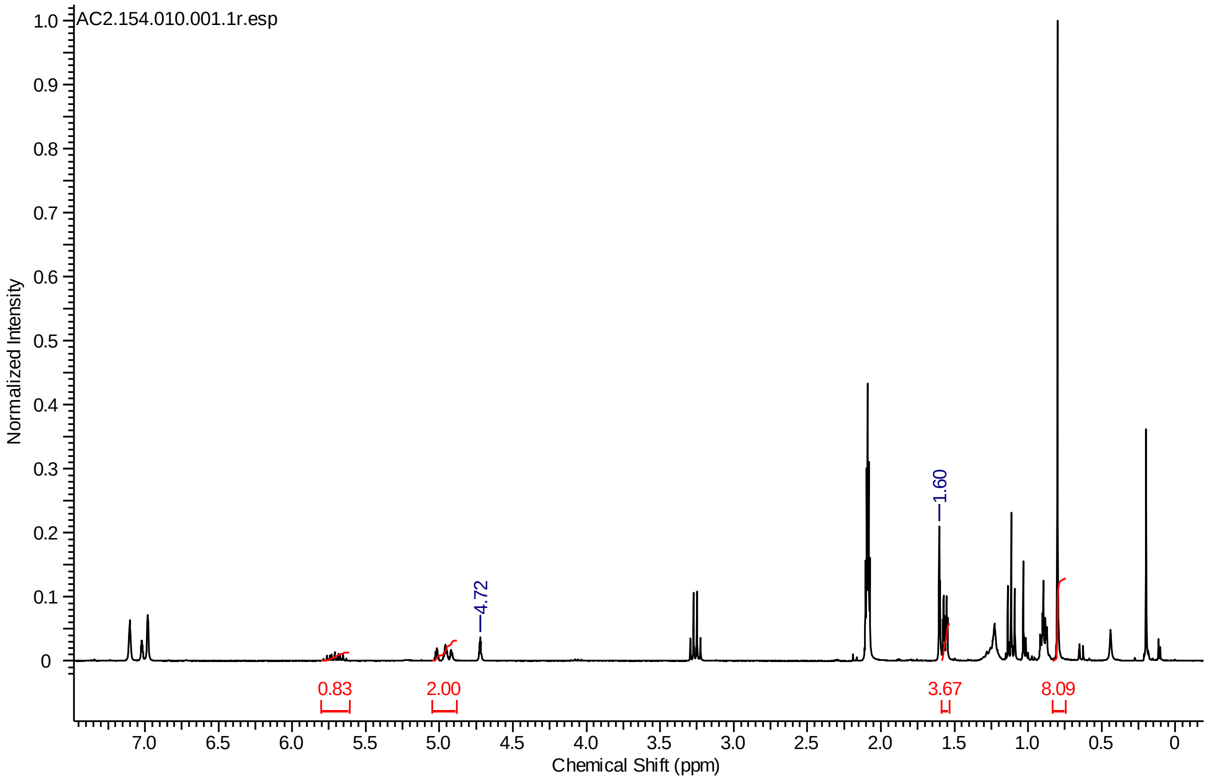

Figure S19: COSY NMR spectrum of the volatile products resulting from the thermal decomposition of compound **5**.

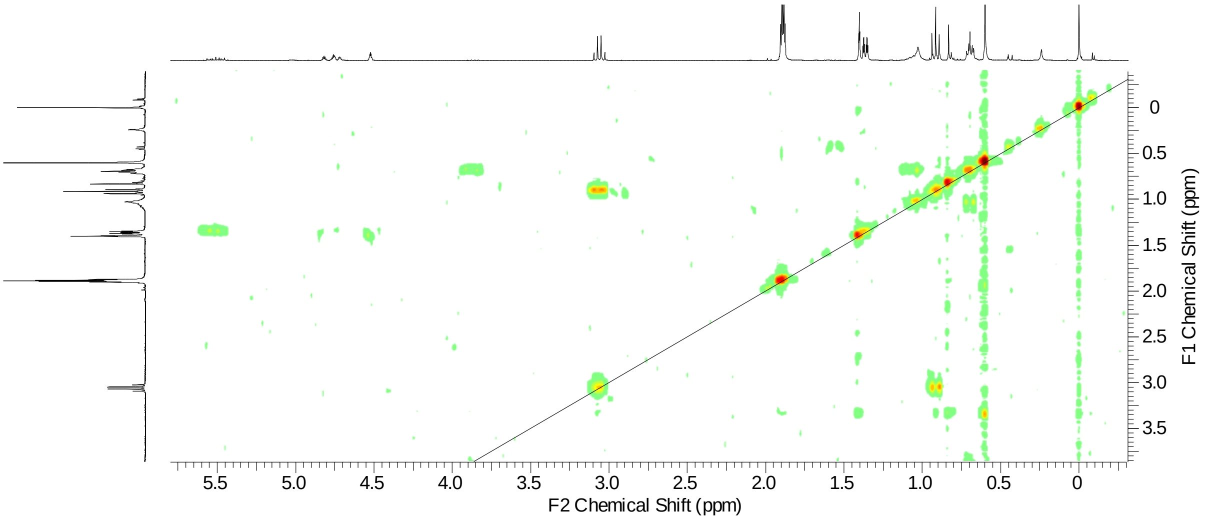

AACVD experiments

Thin films were deposited using a horizontal hot wall reactor. The aerosol was generated using a TSI atomiser and nitrogen was used as a carry gas. Films were grown on 2.5 cm x 15cm SiO_2-coated glass (Pilkington NSG Ltd.) or quartz substrates, which were cleaned with *iso*-propanol, water, acetone and then dried under a flow of nitrogen gas. For each deposition a 0.05 M toluene solution was made up in the glove box and transferred into a bubbler. Depositions were carried out in the temperature range 350-600 °C for a duration of 1 hour.

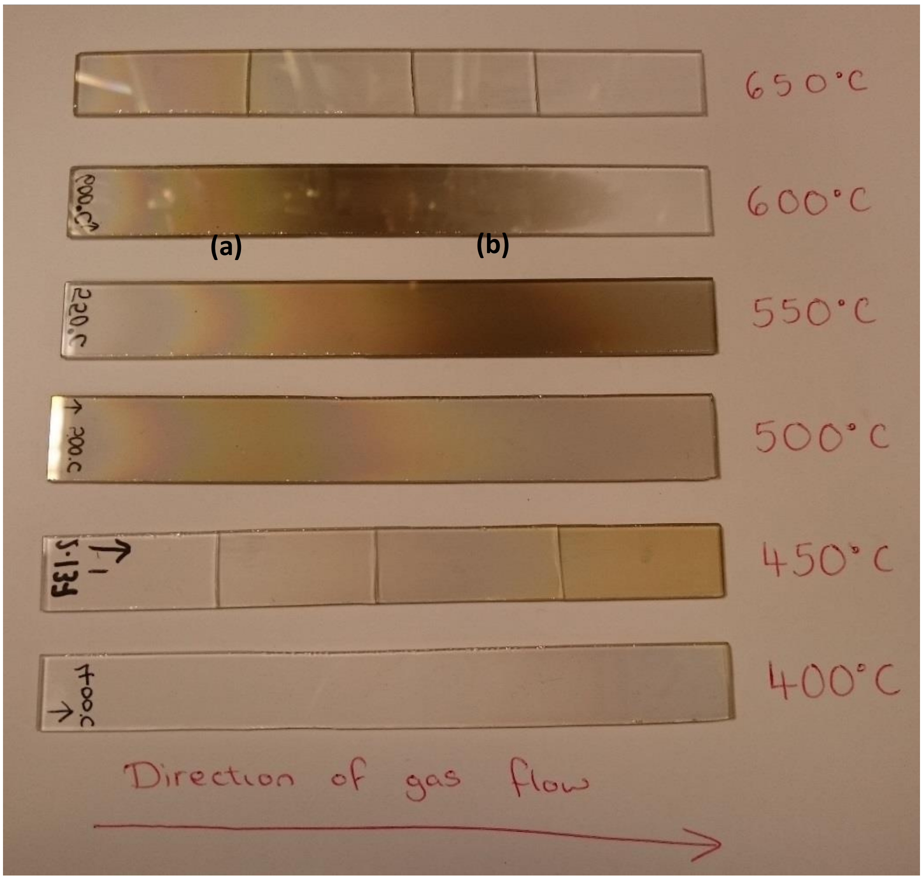

Figure S20: Photo of the as-deposited films deposited on quartz substrates.

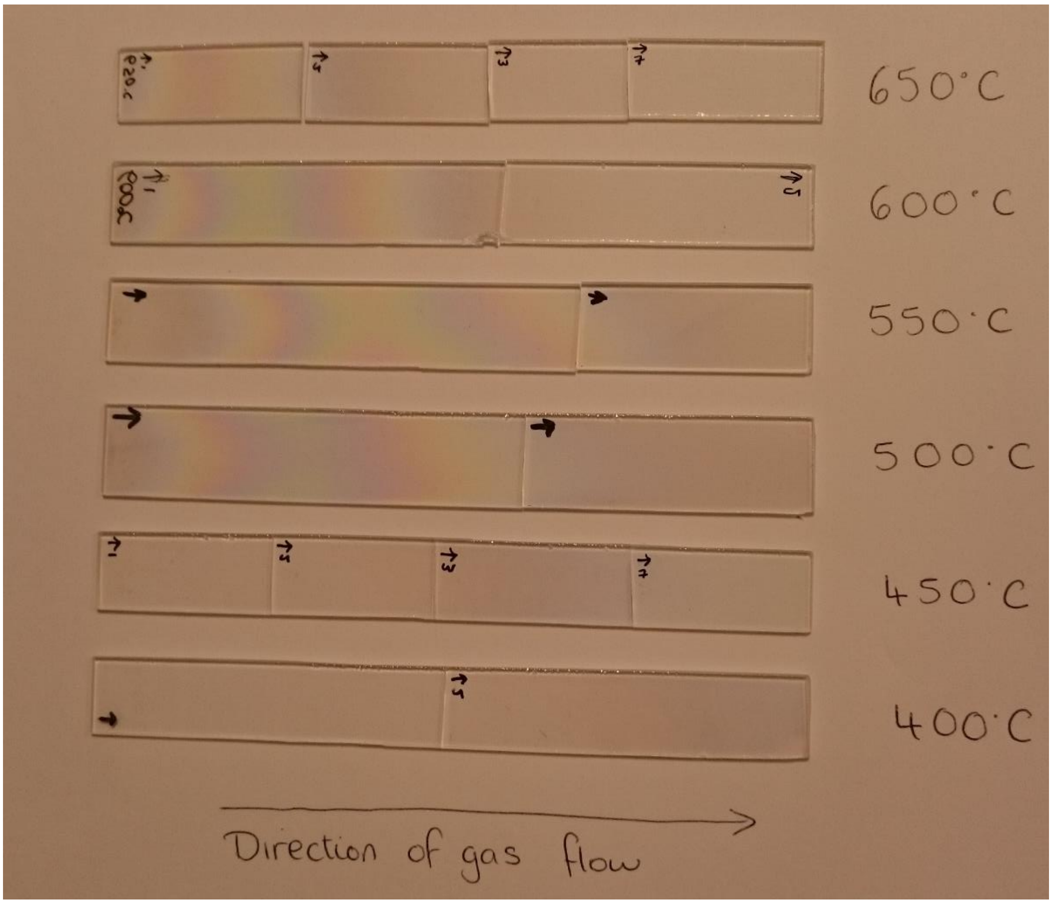

Figure S21: Photo of the film deposited on quartz substrates after annealing at 600 °C for one hour.

SEM and AFM. The morphology of the deposited films was measured by SEM using the FEI NanoSEM 450 and EDAX Octane plus EDS detector with TEAM software and AFM using Nanosurf® easyScan 2 FlexAFM system. AFM analysis was performed using a Digital Instruments Nanoscope IIIa, with BRUKER SNL-10 silicon on nitride lever contact tips (tip radius < 10 nm; f 0 = 50−80 kHz; k = 0.350 N/m; T = 600 nm), in contact mode. Images were processed using the open access Gwyddion SPM data analyser.

UV−Vis−IR Spectroscopy Measurements. UV−vis−IR spectroscopy measurements were collected using a PerkinElmer LAMBDA 750/650 UV−vis and UV−vis−near-IR spectrophotometer. Measurements were recorded at 2000 to 400 nm and zero referenced using 5mm high grade Pilkington-NSG float-glass substrates. The measurements were recorded with 1 nm increments. At 860 nm the PbS

detector switches over to the photomultiplier detector (PMD); as a result a small stepwise noise is generated (±10 nm) within the raw data spectrum.

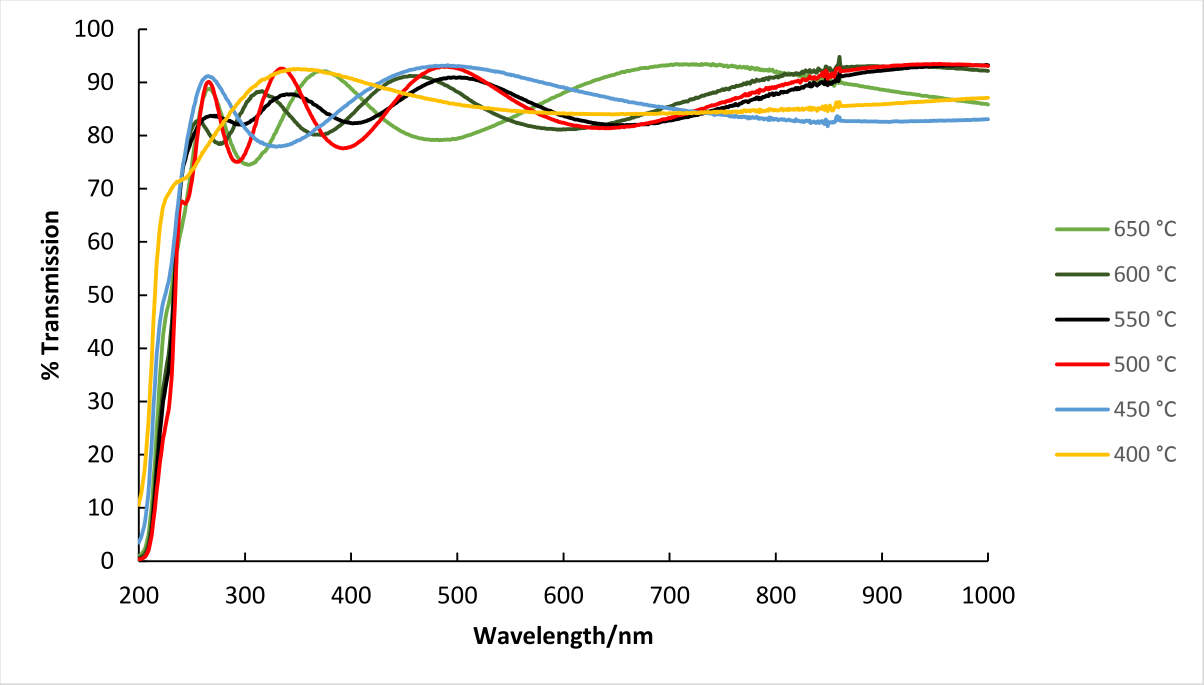

Figure S22:. UV-visible transmission spectra of the annealed thin films grown at various temperatures from complex **6** on quartz substrates.

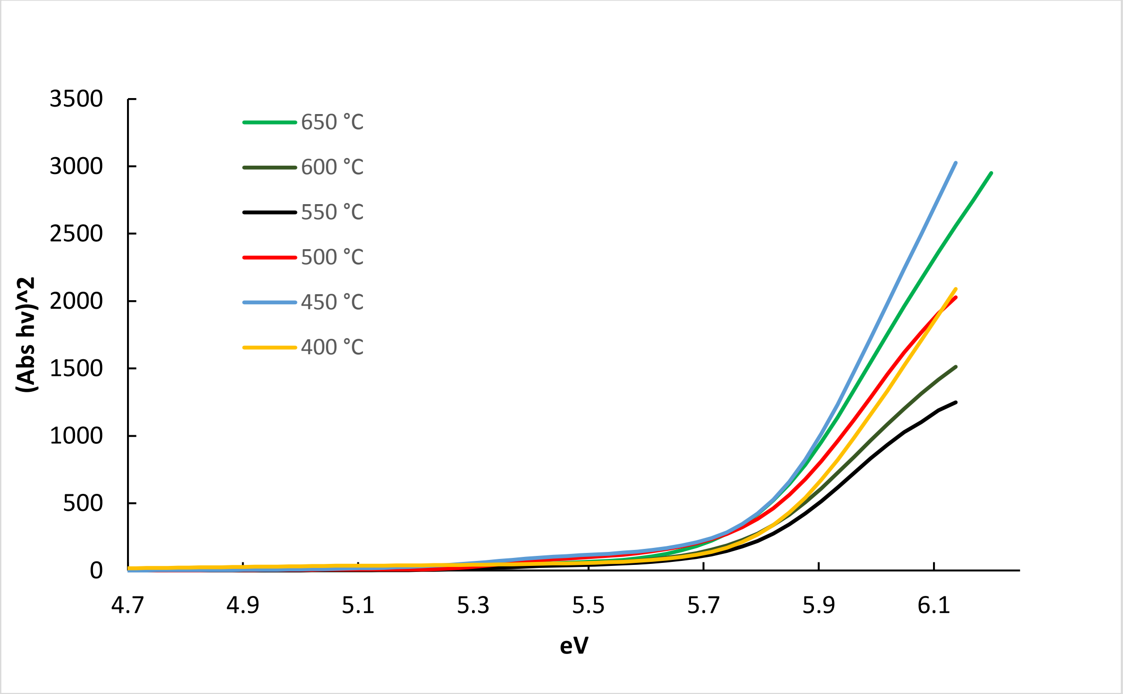

Figure S23: Tauc plots derived from the data shown in Figure S21, indicating the estimated band gaps of the films deposited at various temperatures after annealing at 600 °C.

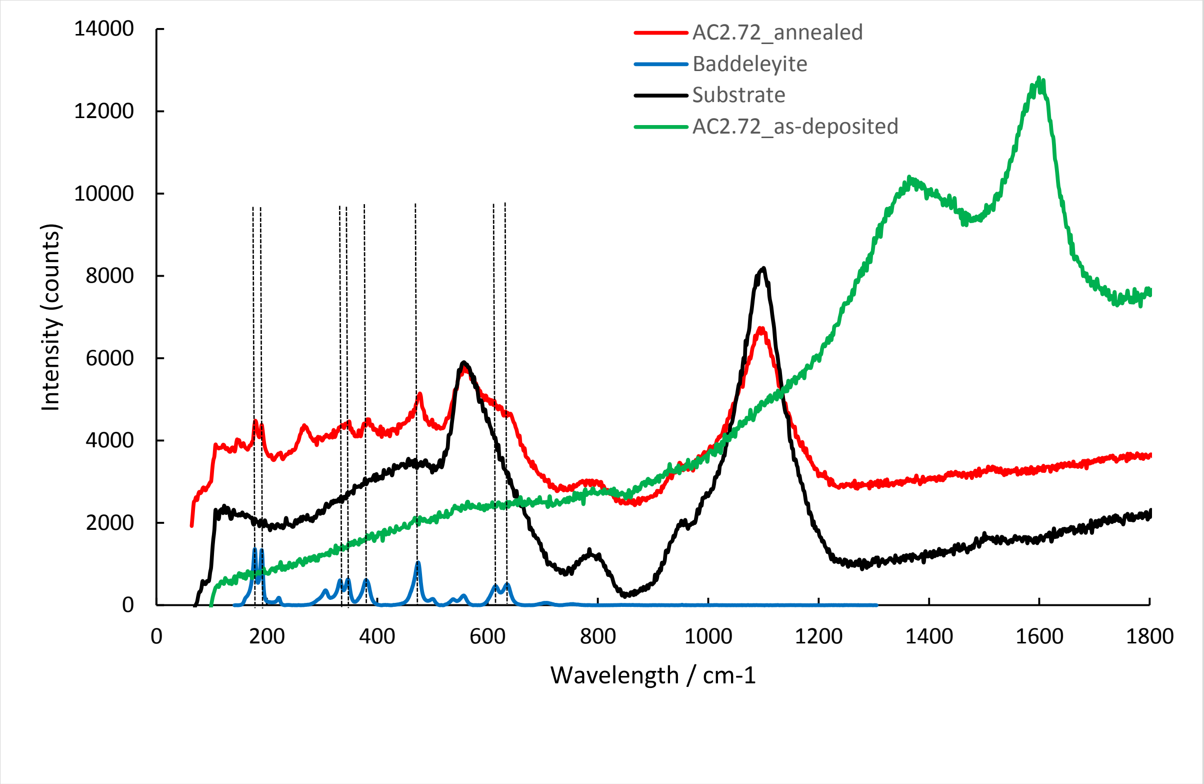

Figure S24: Raman spectra of film deposited at 550 °C

Ellipsometry: The thickness of the annealed films was calculated using ellipsometry using an alpha SE ellipsometer (J.A Woollam Co., Inc. Ellipsometry solutions). The angle of incidence of the beam was 70° to the sample. The resolution of the instrument was (0.2° in delta and psi. The instrument was calibrated using a silicon reference wafer with a 25 nm layer of native oxide. The values of the thickness were determined using Complete Ease software (J.A Woollam Co., Inc.). The results are shown in Figure 4 and Table S1 including estimated errors in the measurements.

Figure S25: Arrhenius plot showing 1000/T versus ln(growth rate) from the data illustrated in Figure 4.

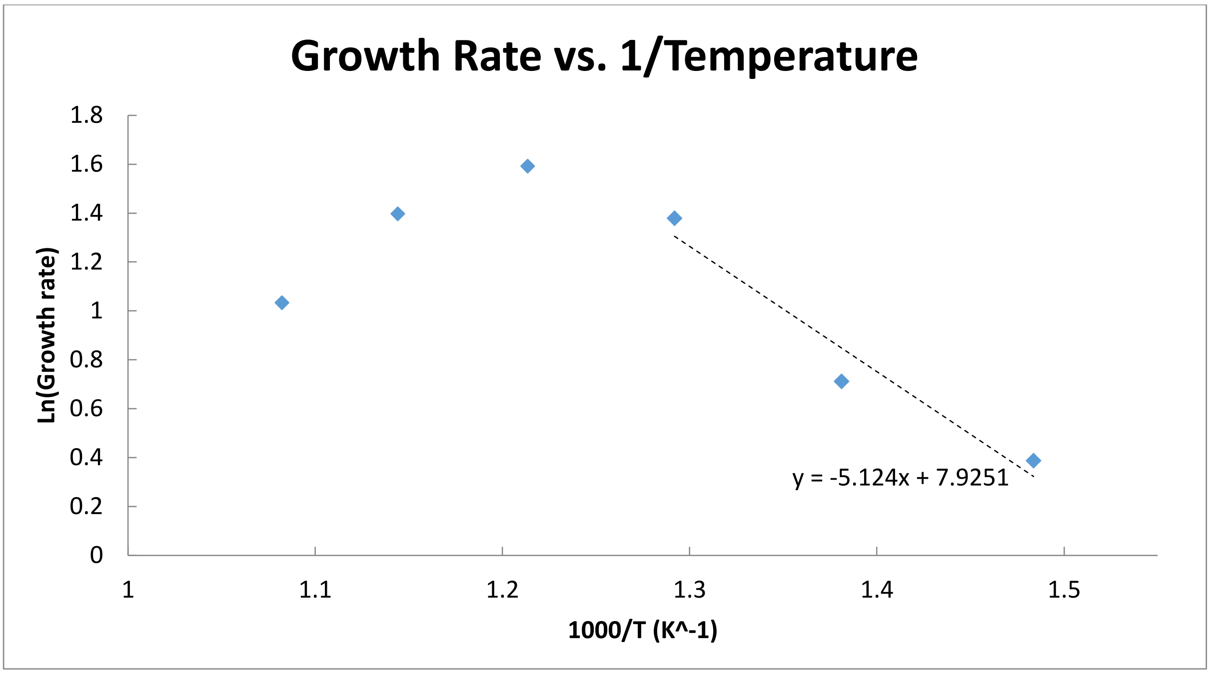

Table S1: Thicknesses of the films annealed at 600 °C determined by ellipsometry.

Temperature	Thickness (nm)	MSE
400	887.31±00.452	25.248
450	122.14±0.454	29.419
500	238.273±0.389	28.273
550	294.53±0.202	13.875
600	242.36±0.17	12.75
650	186.54±0.191	13.293

The activation energy can be calculated using the following relationship:

$$\ln k = \ln A - \frac{E_a}{RT}$$

Where k is the rate constant, A is the pre exponential factor, E_a is the activation energy, R and T are the gas constant and temperature respectively.

X-ray diffraction: In micro-XRD individual particles and small volumes of powder are analysed using a collimated X-ray beam of between 30 and 800 µm in size. Each crystalline phase in the diffractogram is identified by search matching using a database of 300,000 reference patterns.

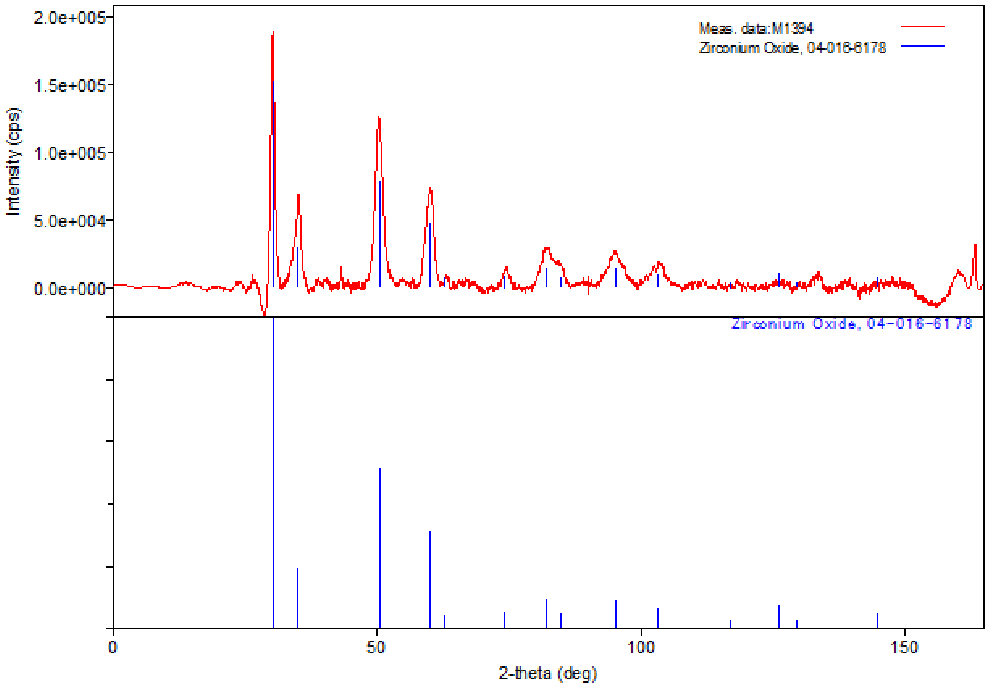

Figure S26: Diffraction pattern for as-deposited ZrO_2 film at 600°C.

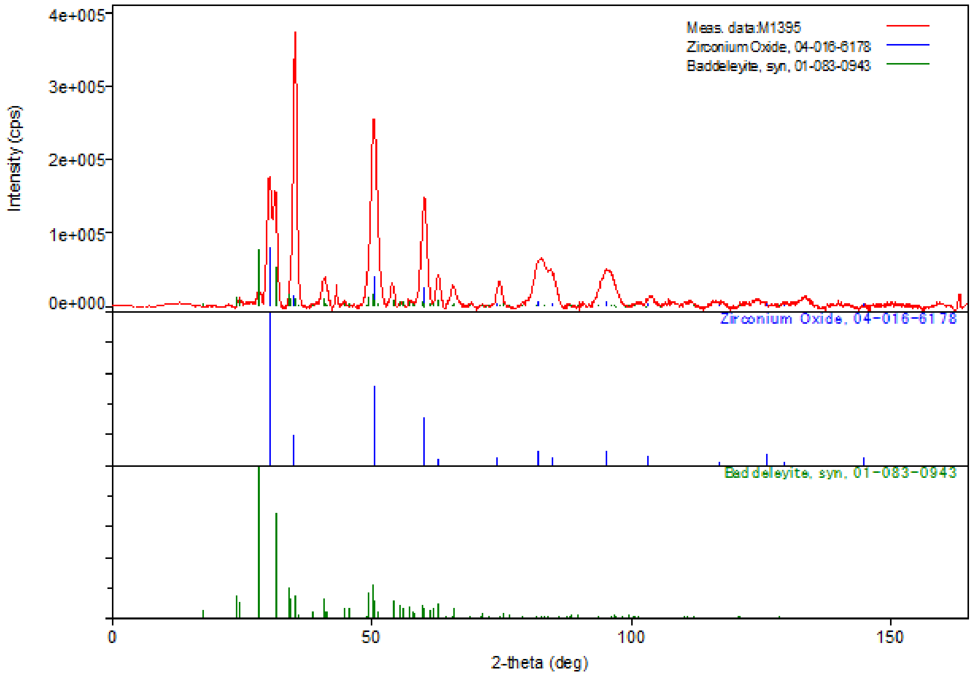

Figure S27: Diffraction pattern for as-deposited ZrO_2 film at 550°C.

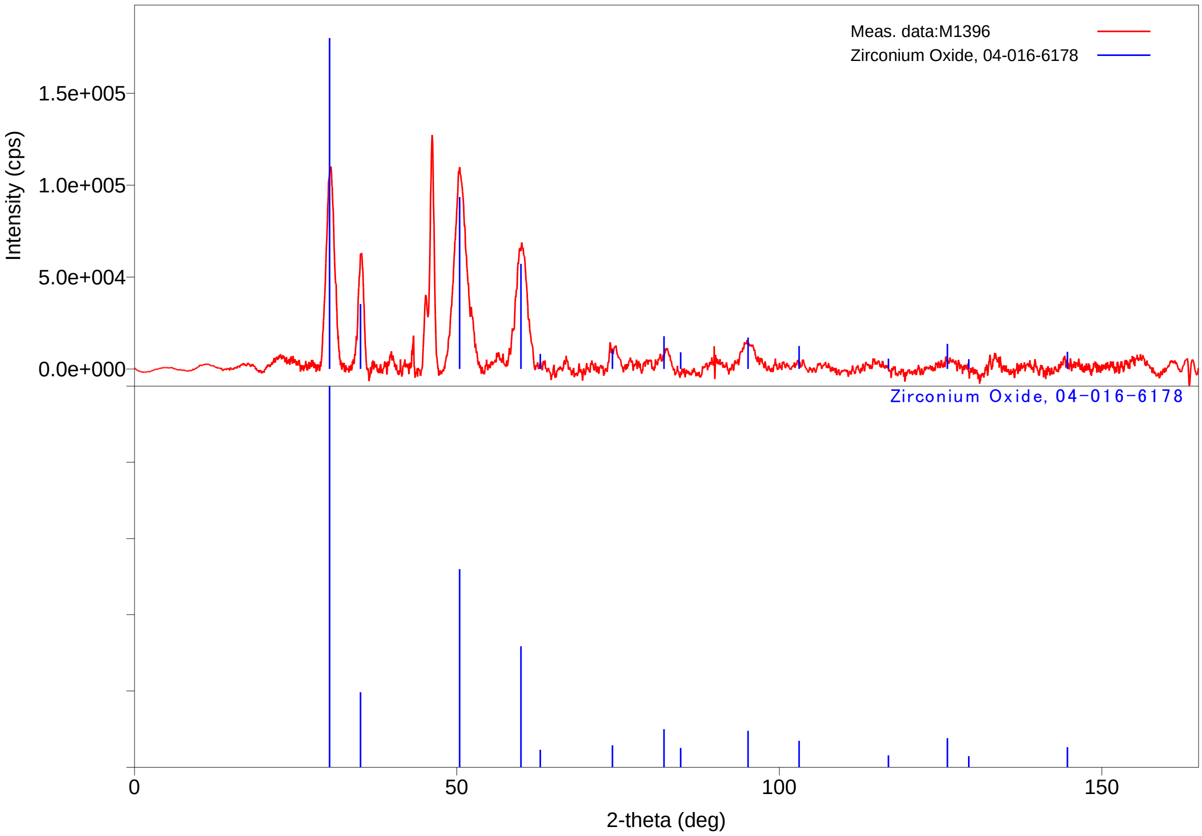

Figure S28: Diffraction pattern for as-deposited ZrO_2 film at 500°C.

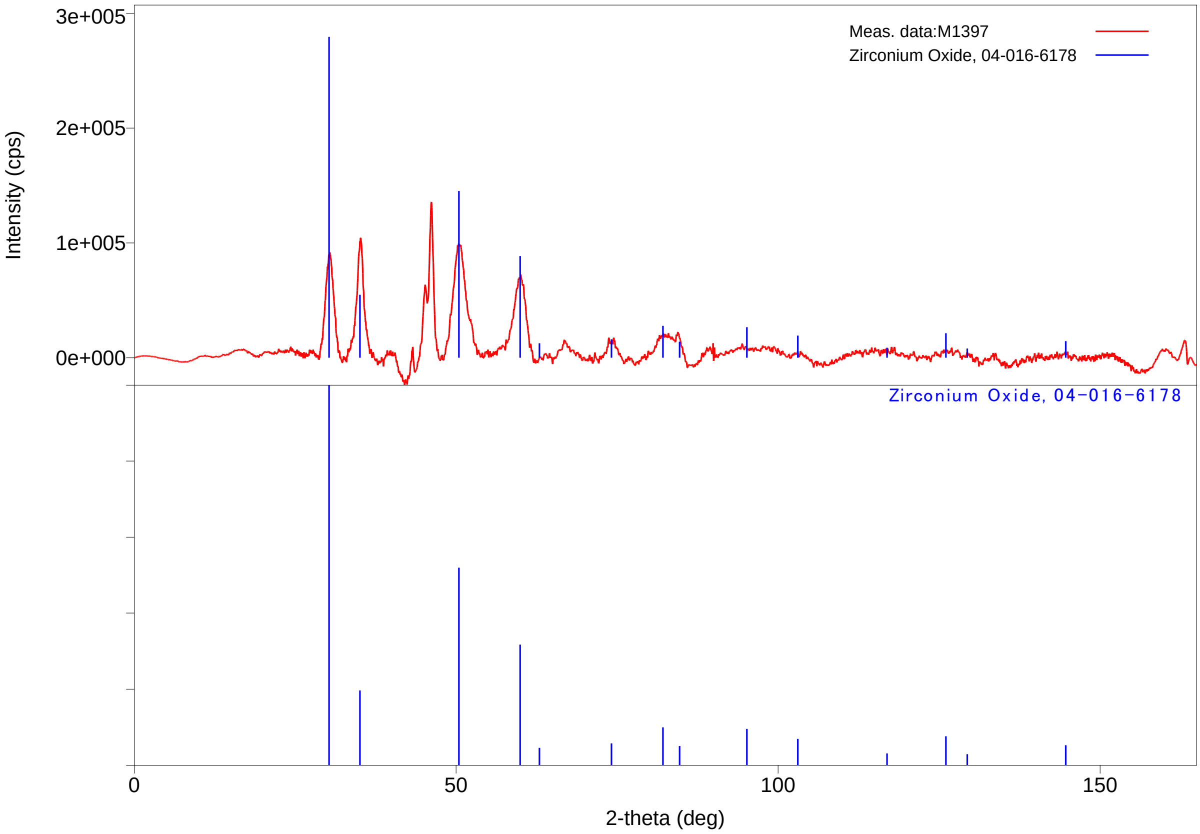

Figure S29: Diffraction pattern for as-deposited ZrO_2 film at 450°C.

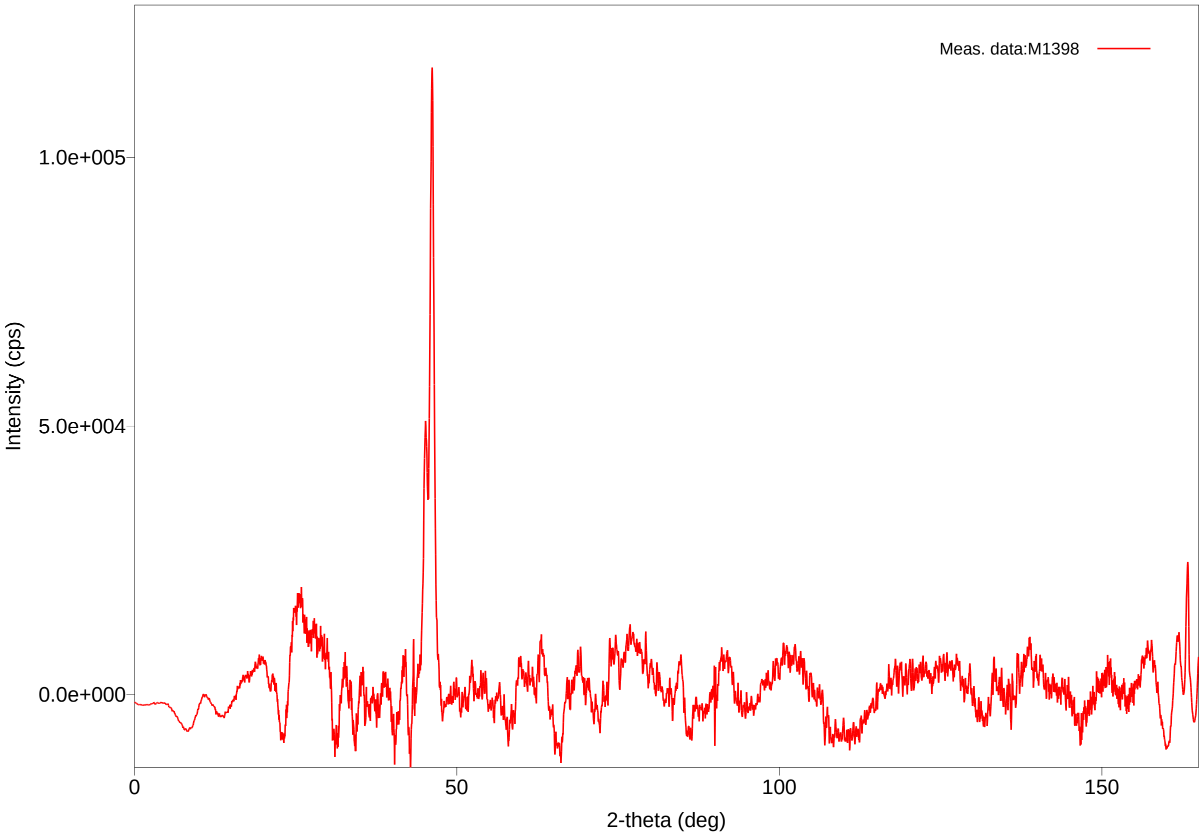

Figure S30: Diffraction pattern for as-deposited ZrO_2 film at 400°C.

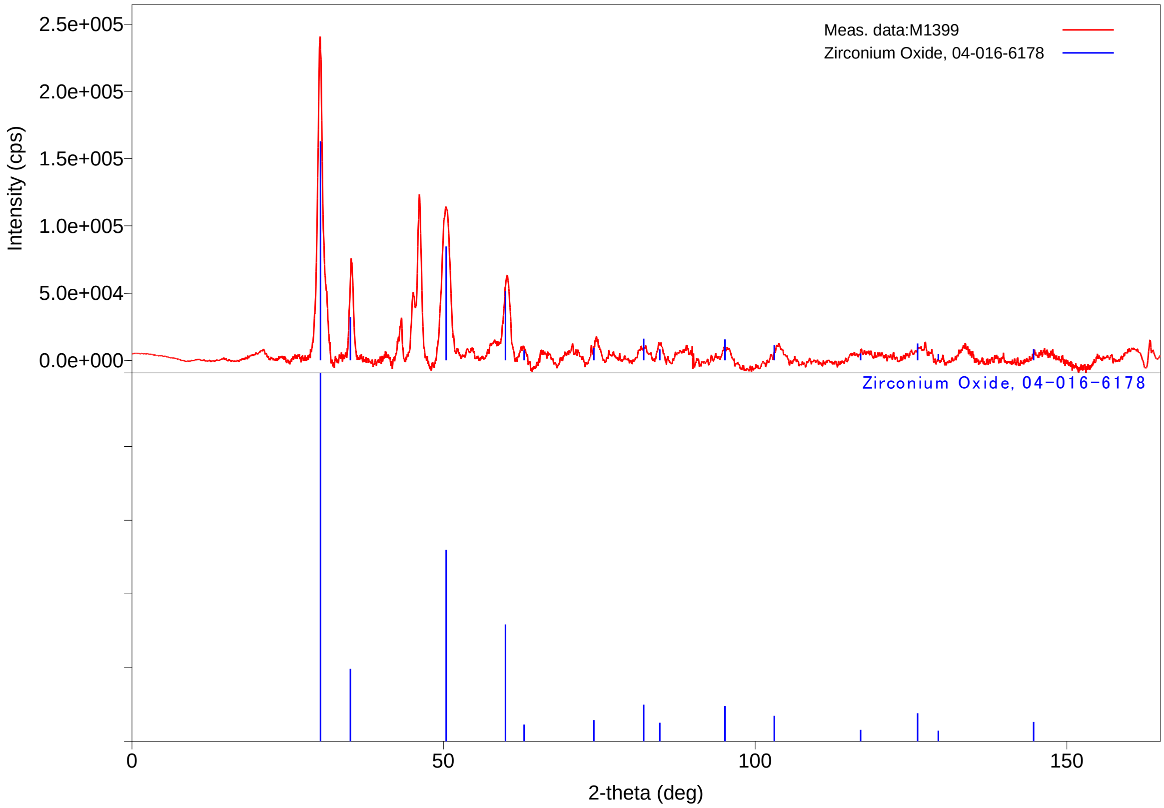

Figure S31: Diffraction pattern for ZrO_2 film deposited at 500°C and annealed in air at 600°C.

X-ray Photoelectron Spectroscopy. XPS measurements for each sample were obtained using Scan mode and in accordance with Test Method RD-I-0612. The argon ion etch beam was operated at 1KeV (M) producing a beam current of 1.56µA and was rastered over a 2.0 x 4.0mm area. A 20 second etch time per level was used with 300 levels of total etching. The X-ray spot size used was 400µm. The binding energy windows used in the acquisition of the profile were: O1s, C1s, Zr3d, Si2p, Ca2p, Na1s and Mg1s. All depth profiles had a very similar appearance with adventitious carbon contamination on the surface of a zirconia coating on silica on glass. There was no carbon detected in the coating or the supposed SiO_2 layer.

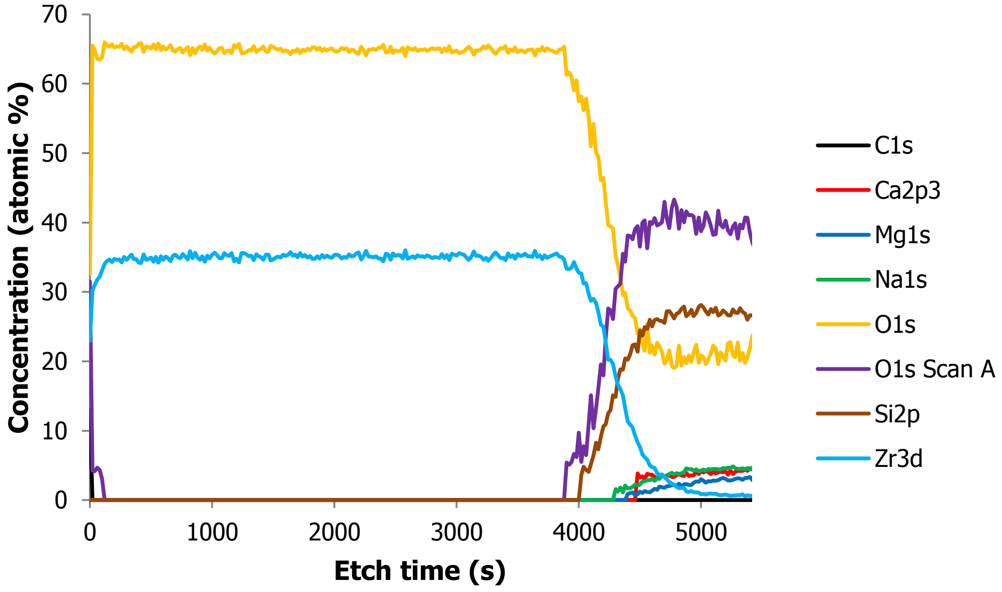

Figure S32: XPS depth profile for ZrO_2 deposited at 500°C.

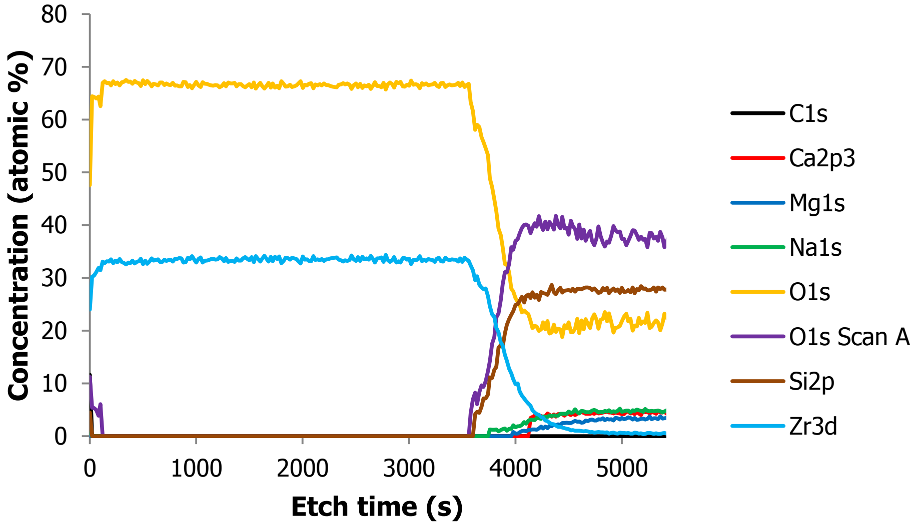

Figure S33: XPS depth profile for ZrO_2 deposited at 500°C and annealed at 600°C.

In order to compare the coatings the oxygen to zirconium ratio was compared throughout the depth of each sample. This comparison is shown in Figure S34. The figure shows that the annealed samples had a stoichiometry much closer to ZrO_2 than the samples that had not been treated at 600°C. The samples that had not been annealed had an average stoichiometry of between $ZrO_{1.8}$ and $ZrO_{1.9}$.

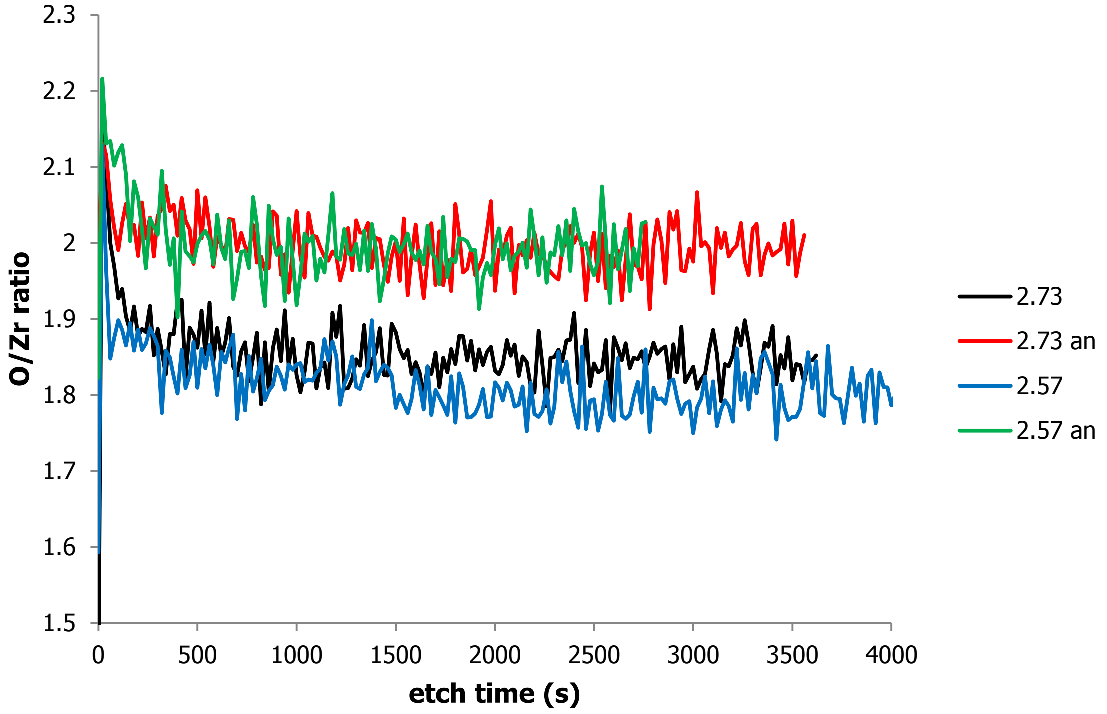

Figure S34: Comparison of the O:Zr ratio across the sample set.

Although no carbon could be quantified in the coatings above the level of XPS background noise it was noticed that the quantification of this background noise was greater for the samples that had not been annealed, suggesting that there may have been more carbon in these samples. In order to qualitatively compare this the 'peak area' over the binding energy range that the C1s peak would usually be quantified was calculated. Figure S35 shows a plot of these data for the entire depth profile of each of the four samples. As with the stoichiometry data there was a clear split in the profile – the two samples that had not been annealed had much larger peak areas, approximately double that of those that had. This suggested that although it was present at concentrations lower than the detection limit of the instrument there was more carbon in the samples that had not been annealed than those which had. This would be in line with the expectation as the additional heat from the annealing process should be enough to remove more organic components within the coating. Similarly, examination of narrow scans of the Zr3d peaks in the XPS data did not reveal any significant difference between the as received and annealed films (Figure S36).

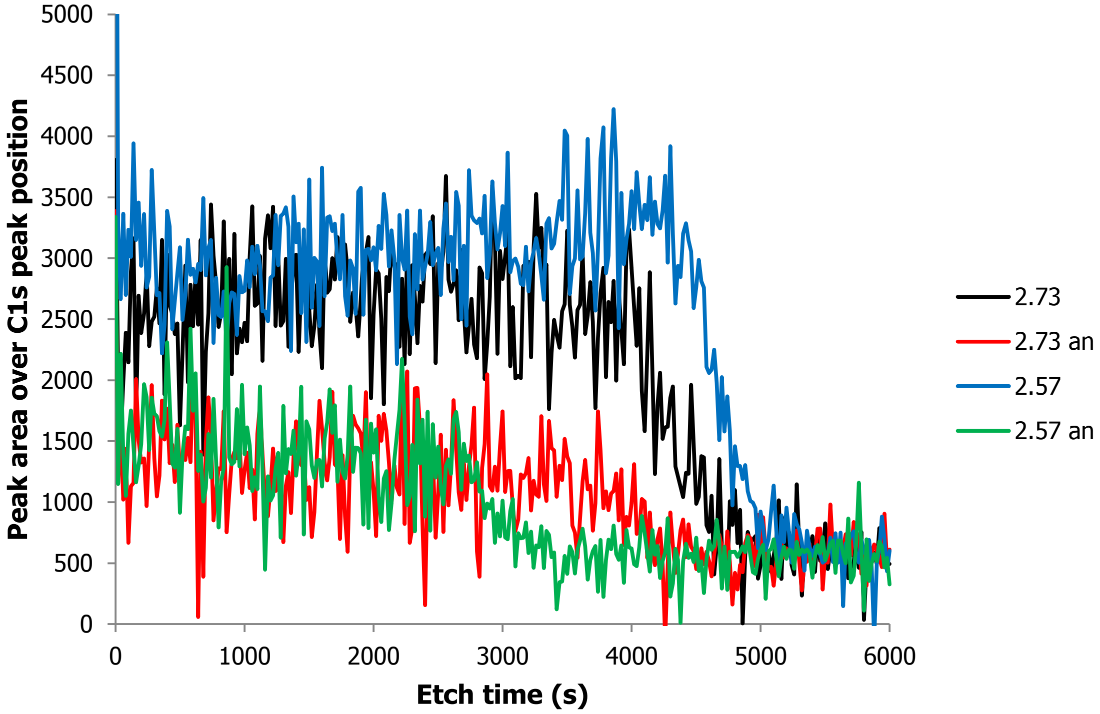

Figure S35: Comparison of the peak area over the expected binding energy range of the C1s peak.

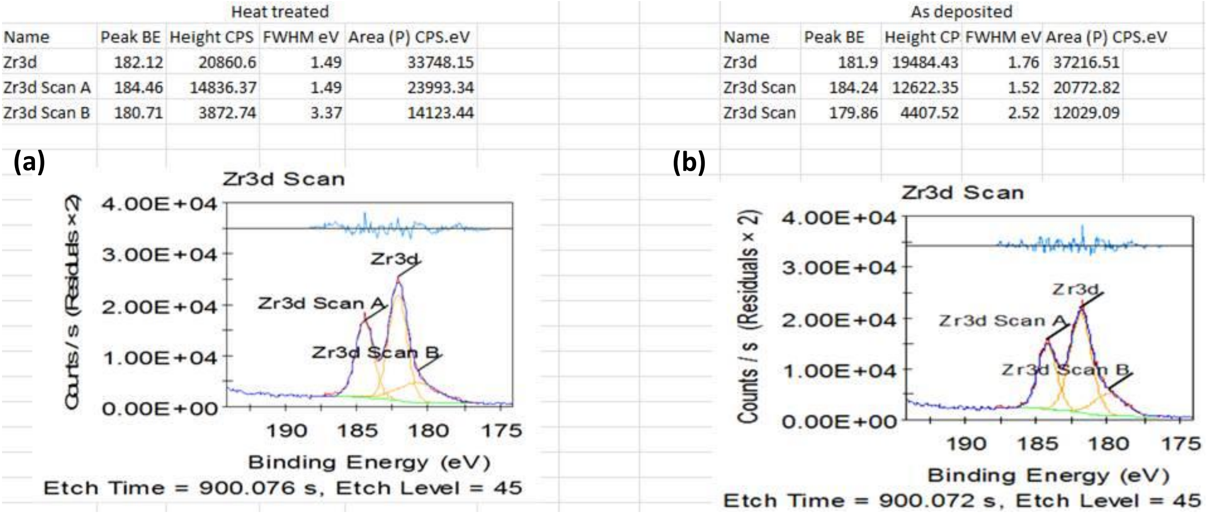

Heat treated

Name	Peak BE	Height CPS	FWHM eV	Area (P) CPS.eV
Zr3d	182.12	20860.6	1.49	33748.15
Zr3d Scan A	184.46	14836.37	1.49	23993.34
Zr3d Scan B	180.71	3872.74	3.37	14123.44

As deposited

Name	Peak BE	Height CP	FWHM eV	Area (P) CPS.eV
Zr3d	181.9	19484.43	1.76	37216.51
Zr3d Scan	184.24	12622.35	1.52	20772.82
Zr3d Scan	179.86	4407.52	2.52	12029.09

Figure 36: Narrow scan comparison of the Zr3d peaks in the XPS data of (a) an as-deposited thin film and (b) a thin film annealed at 600 °C in air. Peaks selected at an arbitrary etch level away from the surface and the glass interface.

Single Crystal X-ray Diffraction Analysis

Data for compound **2** were collected on a Nonius Kappa CCD diffractometer equipped with a low temperature device, using graphite monochromated MoKα radiation (λ= 0.71073 Å). Data were processed using the Nonius Software.[2] Structure solution, followed by full-matrix least squares refinement was performed using the programme suite Olex2 throughout.[3] For compounds **1**, **5** and **6** data were collected on a SuperNova, Dual Cu at zero, EosS2 diffractometer. The crystal was kept at 150(2) K during data collection. Using Olex2,[4] the structures were solved via SHELXS[5] and refined with the ShelXL refinement package using Least Squares minimization. For compound **1** twinning about the 0,0,1 direction accounted for in this refinement. Atoms N4 and C19-C27 exhibited 70:30 disorder about an approximate non-crystallographic mirror containing Zn1 O1 and N3. Comparative chemically equivalent distances were restrained to being similar in both disordered components, as were the ADPs of corresponding atoms pairs. The crystal of compound **5** exhibited classic non-merohedral twinning by virtue of a 180^o rotation about the direct space 1 0 0 vector. Data for both twinned components were integrated simultaneously to account for same. The asymmetric unit of compound **6** comprises 2 crystallographically independent molecules. There was some evidence for non-merohedral twinning in the collected frames of data, and integration as same was pursued. However, as the refined level of twinning refined topped a value of 5%, it was abandoned and the data presented herein reflect integration as a single crystal of the dominant component.

References

1. M. H. Chisholm, C. E. Hammond and J. C. Huffman, *Polyhedron* 1988, **7**, 2515.
2. DENZO-SCALEPACK Otwinowski, Z; Minor, W. "Processing of X-ray Diffraction Data Collected in Oscillation Mode", Methods in Enzymology, Volume 276: Macromolecular Crystallography, part A, p.307-326, **1997**,C.W. Carter, Jr. & R. M. Sweet, Eds., Academic Press.
3. O. V. Dolomanov, L. J. Bourhis, R. J. Gildea, J. A. K. Howard, H. Puschmann, *J. Appl. Cryst*. **2009**, *42*, 339-341.
4. L. J. Bourhis, O. V. Dolomanov, R. J. Gildea, J. A. K. Howard, H. Puschmann, *Acta Cryst. A* **2015**, *71*, 59-75.
5. G. M. Sheldrick, *Acta Cryst. A*, **2008**, *64*, 112-122.